

**Doctoral Dissertation**

**Functional ingredients derived from natural  
products targeting pro-inflammatory lipid  
mediator synthetic pathway**

**2020**

**Keisuke Toda**

***Graduate School of Health & Welfare Science***

***Okayama Prefectural University***

## Contents

<b>Abbreviations .....</b>	<b>2</b>
<b>Chapter I    Introduction .....</b>	<b>4</b>
<b>Chapter II    Ellagitannins from <i>Punica granatum</i> leaves suppress                   microsomal prostaglandin E synthase-1 expression and                   induce lung cancer cells to undergo apoptosis .....</b>	<b>8</b>
MATERIAL AND METHODS .....	10
RESULTS .....	14
DISCUSSION .....	20
<b>Chapter III   Red-kerneled    rice    proanthocyanidin    inhibits                   arachidonate 5-lipoxygenase and decreases psoriasis-like                   skin inflammation .....</b>	<b>22</b>
MATERIAL AND METHODS .....	24
RESULTS .....	31
DISCUSSION .....	39
<b>Chapter IV    Conclusion Remarks .....</b>	<b>42</b>
<b>Acknowledgement .....</b>	<b>45</b>
<b>References .....</b>	<b>46</b>

## Abbreviations

Bcl-2	B-cell chronic lymphocytic leukemia/lymphoma 2
COX	cyclooxygenase
cPGES	cytosolic prostaglandin E synthase
CRE	cAMP response element
DAPI	4',6-diamidino-2-phenylindole
DHHP	dehydrohexahydroxydiphenyl
DMSO	dimethyl sulfoxide
ESI-MS	electrospray ionization mass spectrometry
Et <sub>2</sub> O	diethyl ether
EtOAc	ethyl acetate
GAPDH	glyceraldehyde 3-phosphate dehydrogenase
HE	hematoxylin and eosin
HEK	human embryonic kidney
HETE	hydroxyeicosatetraenoic acid
HPETE	hydroperoxyeicosatetraenoic acid
IL	interleukin
IMQ	imiquimod
iNOS	inducible nitric oxide synthase
KPB	potassium phosphate buffer
Krt1	keratin 1
LOX	lipoxygenase

LT	leukotriene
mPGES-1	microsomal prostaglandin E synthase-1
mPGES-2	membrane-bound prostaglandin E synthase-2
MRM	multiple reaction monitoring
<i>n</i> -BuOH	water-saturated <i>n</i> -butanol
NF-κB	nuclear factor-κB
NSAIDs	non-steroidal anti-inflammatory drugs
PG	prostaglandin
RBL	rat basophilic leukemia
RRP	red-kerneled rice proanthocyanidin
Th17	T helper 17
TNF	tumor necrosis factor
TUNEL	terminal deoxynucleotidyl transferase-mediated dUTP nick end labeling

# **Chapter I**

## **Introduction**

Japan has been a super-aged society with more than 21% of the population of 65 years or older. Chronic diseases that increase with aging are triggered by the underlying chronic inflammation. Therefore, the key to a long and healthy life is to prevent chronic inflammation.

Prostaglandin (PG)  $E_2$  and leukotrienes (LTs) play a key role in pro-inflammation.  $PGE_2$  is widely distributed in many tissues and organs, and contributes to maintenance of homeostasis such as awakening, bone metabolism, and inhibition of gastric secretion. On the other hand, it regionally causes or promotes various pathophysiological reactions including fever, pain, and tumorigenesis<sup>1-4</sup>.  $PGE_2$  is biosynthesized from arachidonic acid by cyclooxygenase (COX) and PGE synthase (PGES)<sup>1</sup>(Fig. 1). The COX-2 and microsomal PGES-1 (mPGES-1) are functionally coupled<sup>5</sup> and induced by pro-inflammatory cytokines, growth factors, and endotoxins. Subsequently, the hyperproduced  $PGE_2$  causes several inflammatory disorders<sup>6</sup>.

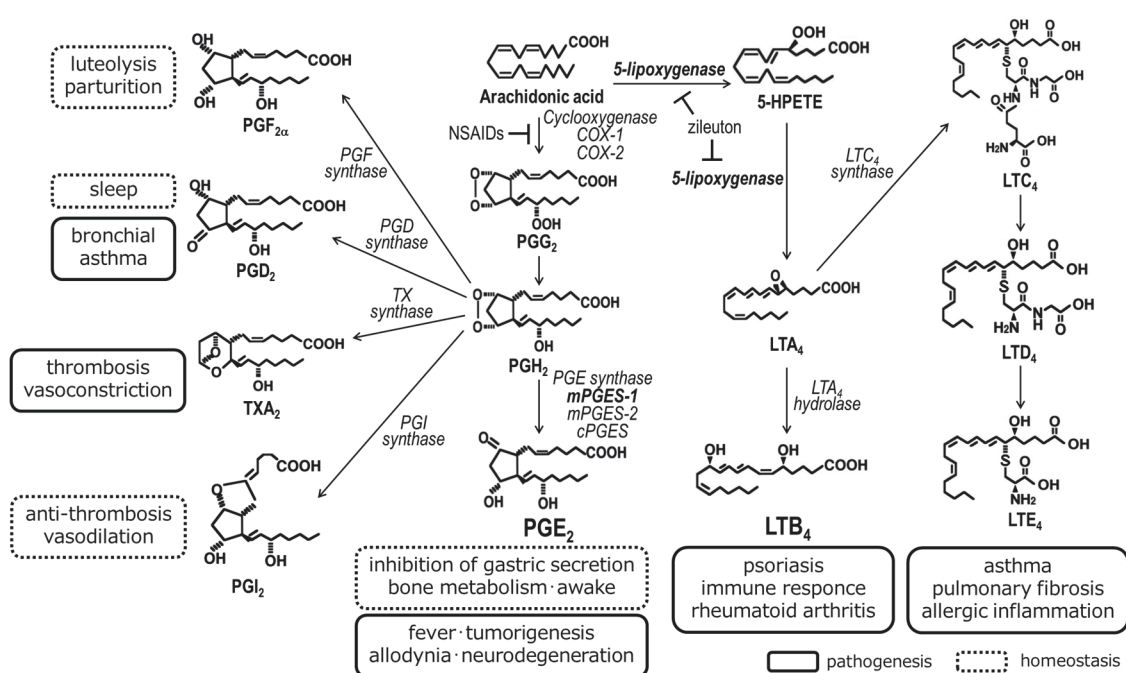


**Fig. 1. Arachidonic acid cascade.**

These lipid mediator bind to specific receptors and exerts various physiological effects.

In clinical treatment, COX inhibitors called non-steroidal anti-inflammatory drugs (NSAIDs) are used widely as antipyretic analgesic drugs. However they have side effects, because they reduce not only pathogenetic PGE<sub>2</sub> but also the other important prostanoids for maintaining homeostasis. Though COX-2 selective inhibitors have been developed to reduce the side effects, even they increase the risk of cardiovascular disease, because COX-2 inhibition in vascular endothelial cells reduces PGI<sub>2</sub> as an anti-platelet aggregation factor <sup>7-9</sup>. In fact, it is demonstrated experimentally that COX-2-deficient mice, but not mPGES-1-deficient mice, show accelerated thrombogenesis and elevated blood pressure <sup>10</sup>. Thus, there is a strong demand for development of an effective and safe alternative approach to use of COX inhibitors, and mPGES-1 is thought to represent a possible therapeutic target for inflammatory disorders <sup>2</sup>. Previously it was demonstrated that *Dioscorea japonica* extract reduced PGE<sub>2</sub> production in cancer and inflammatory cells<sup>11</sup>, and exhibited the preventive effects on skin carcinogenesis <sup>12</sup>, however, the effects were resulted by the suppressed COX-2 and mPGES-1 expression. Furthermore, it will be important to explore substances specifically targeting mPGES-1 from natural products.

5-lipoxygenase (LOX) is a key enzyme in the production of LTs, and dual-functionally catalyzes the oxygenation of arachidonic acid to 5-hydroperoxyeicosatetraenoic acid (5-HPETE) and its dehydration to LTA<sub>4</sub> (Fig. 1). LTA<sub>4</sub> is then converted to LTB<sub>4</sub> by LTA<sub>4</sub> hydrolase and LTC<sub>4</sub> by LTC<sub>4</sub> synthase. LTB<sub>4</sub> promotes chemotaxis and activates leukocytes, whereas LTC<sub>4</sub> and the metabolites LTD<sub>4</sub> and LTE<sub>4</sub> are involved in bronchoconstriction, mucus secretion, and in the pathogenesis of asthma. Zileuton, the only 5-LOX inhibitor presently available for clinical use, has side effects such as liver toxicity <sup>13,14</sup>. Therefore, novel inhibitors of 5-LOX without side effects are needed to improve and prevent chronic inflammatory disorders including psoriasis.

In this study, functional ingredients derived from natural products targeting mPGES-1 and 5-LOX were explored. Chapter II describes that ellagitannins from *Punica granatum* leaves down-regulated mPGES-1 expression in human non-small cell lung carcinoma A549 cells, and induced cancer cells to apoptosis <sup>15</sup>. Chapter III describes that red-kerneled rice proanthocyanidin (RRP) inhibited mPGES-1 and 5-LOX, and improved the psoriasis-like skin inflammation <sup>16</sup>.



## **Chapter II**

**Ellagitannins from *Punica granatum* leaves  
suppress microsomal prostaglandin E  
synthase-1 expression and induce lung  
cancer cells to undergo apoptosis**

*Punica granatum*, known commonly as pomegranate, and various parts of this plant are used in traditional medicine. For example, in Chinese medicine, the pericarps are used as antidiarrhetic, hemostatic, and vermifuge agents; in Unani medicine, the flowers are used as a dietary supplement to treat diabetes <sup>17</sup>; and, in Ayurvedic medicine, the bark and roots are considered to have anthelmintic properties <sup>18</sup>. Moreover, there are a few reports of pomegranate leaves having anti-inflammatory effects <sup>19,20</sup>; however, the active substances and the mechanism of action are not yet fully understood.

In this study, it was demonstrated that granatin A and granatin B, abundant in pomegranate leaves, and the structural analog, geraniin, specifically down-regulated mPGES-1 expression, and they had effects on inflammation and carcinogenesis in human lung carcinoma model A549 cells.

## MATERIALS AND METHODS

### *Preparation of extract and ellagitannins*

70% aqueous acetone extract of *Photinia × fraseri*, *Siraitia grosvenorii*, *Punica granatum* leaf, and *Magnolia coco*, and ellagitannins were kindly provided by Prof. Hideyuki Ito. The ellagitannins were extracted by reference to previous reports <sup>21,22</sup>. Pomegranate leaves (590 g) were homogenized with 70% aqueous acetone, and the homogenate was filtered and concentrated to obtain the acetone extract (150 g). A part of the acetone extract (20 g) was extracted with diethyl ether (Et<sub>2</sub>O), ethyl acetate (EtOAc), and water-saturated *n*-butanol (*n*-BuOH) each 1.8 L to yield the Et<sub>2</sub>O extract (163 mg), EtOAc extract (6.1 g), *n*-BuOH extract (5.8 g), and water soluble portion (5.6 g). The EtOAc extract was column chromatographed over TOYOPEARL® HW-40 (Tosoh Co., Tokyo, Japan), yield granatin A (252 mg, 98.3% purity) and granatin B (3.3 g, 97.1% purity). Geraniin (97.0% purity) was isolated using the method described previously <sup>23</sup>. The dried extracts and ellagitannins were re-dissolved in dimethyl sulfoxide (DMSO) or ethanol and added to the cell culture medium.

### *Cell culture*

The human non-small cell lung carcinoma cell line A549 (ATCC CCL-185) was obtained from RIKEN BioResource Center (Tsukuba, Japan). The cells were cultured in Dulbecco's modified Eagle's medium (DMEM) containing 10% fetal bovine serum, 100 units/ml penicillin, and 100 µg/ml streptomycin. The cells were maintained at 37 °C in a humidified atmosphere of 95% air and 5% CO<sub>2</sub>. A549 cells treated with 0–10 µg/ml

acetone extract or 0–10  $\mu$ M granatin A, granatin B, and geraniin in ethanol, or the other extracts in DMSO or were added only vehicle as a control. The viability of the cells was measured using the CellTiter-Glo<sup>®</sup> 2.0 Assay (Promega, Madison, WI. USA).

### ***Real-time quantitative PCR***

After 24 h treatment in either the presence or absence of 10 ng/ml IL-1 $\beta$ , A549 cells were collected, the total RNA was isolated using the acid guanidinium thiocyanate procedure, and cDNA was prepared using the High-Capacity cDNA Reverse Transcription Kit (Applied Biosystems, LLC, Foster City, CA. USA). Real-time PCR was performed using SsoAdvanced<sup>™</sup> Universal SYBR<sup>®</sup> Green Supermix (Bio Rad Labs., Hercules, CA. USA) on the StepOnePlus<sup>™</sup> Real-Time PCR System (Applied Biosystems, LLC, Foster City, CA. USA), and primer pairs, as follows: *PTGES* (mPGES-1), 5'-TGATCACACCCACAGTTGAGC-3' (forward) and 5'-TGATGATGGCCACCACGTA-3' (reverse); *PTGS2* (COX-2), 5'-TGCATTCTTTGCCCAGCACT-3' (forward) and 5'-AAAGGCGCAGTTTACGCTGT-3' (reverse); *TNF* (TNF $\alpha$ ), 5'-GGACCTCTCTCTAA TCAGCCCTC-3' (forward) and 5'-TCGAGAAGATGTCTGACTGCC-3' (reverse); *NOS2* [inducible nitric oxide synthase (iNOS)], 5'-TGCAGACACGTGCGTTACTCC-3' (forward) and 5'-GGTAG CCAGCATAGCGGATG-3' (reverse); *BCL2* [B-cell chronic lymphocytic leukemia/lymphoma 2 (Bcl-2)], 5'-AGTACCTGAACCGGCACCT-3' (forward) and 5'-GCCGTACAGTTCCACAAAGG-3' (reverse); *GAPDH* [glyceraldehyde 3-phosphate dehydrogenase (GAPDH)], 5'-CGAGATCCCTCCAAAA TCAA-3' (forward) and 5'-TTCACACCCATGACGAACAT-3' (reverse). The data were normalized to the *GAPDH* expression level.

### ***Western blotting***

Microsomal fractions (20 µg) from A549 cells, treated for 48 h either with or without 10 ng/ml IL-1β were electrophoresed on SDS-polyacrylamide gels and then transferred them onto Immobilon-P membrane (Millipore, Burlington, MA. USA). Following treatment with blocking reagent (Roche, Penzberg, Germany), the membrane was incubated with either rabbit anti-mPGES-1 IgG (1:1000, Novus Biologicals, LLC, Centennial, CO. USA), rabbit anti-COX-2 IgG (1:100, Immuno-Biological Laboratories Co., Ltd., Gumma, Japan) or rabbit anti-β-actin IgG (1:1000, Cell Signaling Technology, Boston, MA. USA). It was visualized the immunoreactive proteins using BM chemiluminescence Western blotting kit (Roche). The densities of each of the protein bands were assessed as described previously <sup>11</sup>.

### ***mPGES-1 activity***

The cells were incubated for 24 h in either the presence or absence of 10 ng/ml IL-1β, 10 µM granatin A or granatin B, or geraniin, as indicated. After the cells were scraped off the dishes and disrupted by sonication, the microsomal fractions were isolated by centrifugation at 100,000 xg. The microsomal fractions were used as the enzyme source. mPGES-1 activity was initiated by adding 40 µM PGH<sub>2</sub> in 100 mM KPB buffer (pH 7.2) with 2.5 mM glutathione for 1 min at 24 °C. The reaction was terminated using 100 mM FeCl<sub>2</sub> / 0.5 M citric acid, and 2.5 nmol of PGB<sub>2</sub> were added as an internal standard. The PGE<sub>2</sub> produced was analyzed via reverse-phase HPLC using COSMOSIL 5C18-MS-II column (5 µm particle, 4.6×250 mm, Nacalai Tesque, Kyoto, Japan) with a solvent system of acetonitrile/water/acetic acid (40:60:0.01, v/v). The absorption spectrum was monitored at 192 nm continuously, using the Waters 2489 UV/Visible

detector. The PGE<sub>2</sub> was quantified by comparing of the peak areas with that of an internal standard.

### ***Enzyme immunoassay***

Following 24 h treatment to A549 cells ( $2 \times 10^4$  cells/well) either with or without 10 ng/ml IL-1 $\beta$ , 10  $\mu$ M granatin A or granatin B, or geraniin, arachidonic acid (10  $\mu$ M) was added to the culture medium of the cells. After 30 min incubation with the arachidonic acid, PGE<sub>2</sub> concentration was measured in the medium via an enzyme immunoassay using the PGE<sub>2</sub> ELISA Kit (Cayman Chemical Co. Ann Arbor, MI. USA), according to the manufacturer's instructions.

### ***TUNEL assay***

After 48 h treatment by the above concentrations of the ellagitannins, terminal deoxynucleotidyl transferase-mediated dUTP nick end labeling (TUNEL) assay was carried out to identify the extent of DNA fragmentation in the A549 cells, using the Peroxidase *In Situ* Apoptosis Detection Kit (EMD Millipore, Billerica, MA. USA), as described previously<sup>11</sup>. The number of TUNEL-positive cells was counted in 10 separate observations with a light microscope (ECLIPSE 80i; Nikon Co., Tokyo, Japan).

### ***Statistics***

The data were analyzed statistically using Dunnett's post-hoc test at a significance level of  $p < 0.01$ .

## RESULTS

COX-2 and mPGES-1 are expressed constitutively in lung carcinoma A549 cells, and approximately 10-fold and 20-fold expression was induced by IL-1 $\beta$  (data not shown). In IL-1 $\beta$  stimulated A549 cells, mPGES-1 suppression of some samples derived from natural products was screened, and pomegranate leaf extract showed the dose-dependent effect without COX-2 suppression among them. (Fig. 2). Pomegranate leaf extract (acetone extract) suppressed the expression of mPGES-1 in a dose-dependent manner (0–10  $\mu$ g/mL); however, it tended to induce COX-2 expression in the cells (Fig. 3A). Then, the sequent some fractions extracted by the liquid–liquid method described in the Materials and Methods section and in Fig. 3D. Following addition of each fraction (10  $\mu$ g/ml) to the culture medium of A549 cells, the EtOAc and *n*-BuOH fractions suppressed mPGES-1 expression strongly in a dose-dependent manner (Fig. 3B and C). The

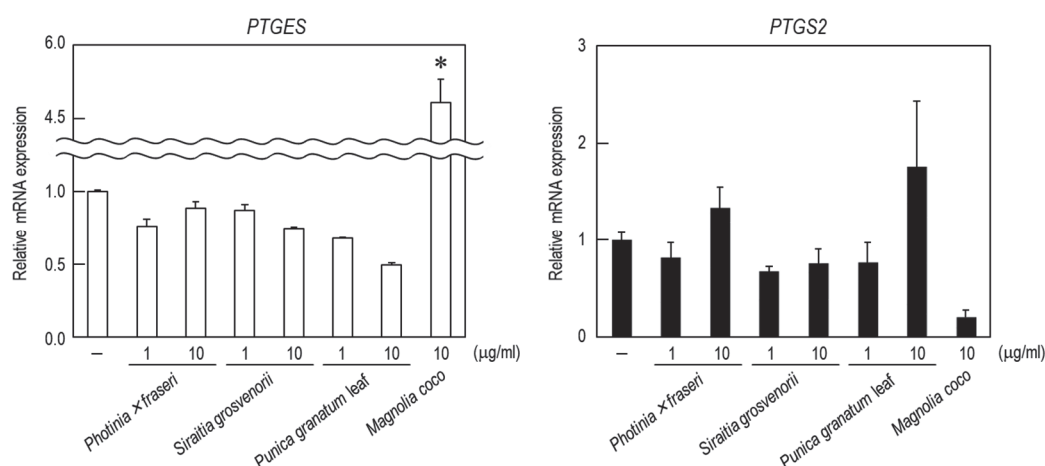


**Fig. 2. Screening for suppression of *PTGES* (mPGES-1) expression in A549 cells.**

Changes in mRNA levels of *PTGES* (open bar) and *PTGS2* (closed bar) by treatment with acetone extract of *Photinia x fraseri*, *Siraitia grosvenorii*, *Punica granatum* leaf, and *Magnolia coco* were analyzed by real-time PCR, as described in the Materials and Methods section. The values are represented as a relative value against control without extract treatment and represent mean  $\pm$  SEM ( $n = 3$ ). \* $p < 0.01$ , compared with control without extract treatment.

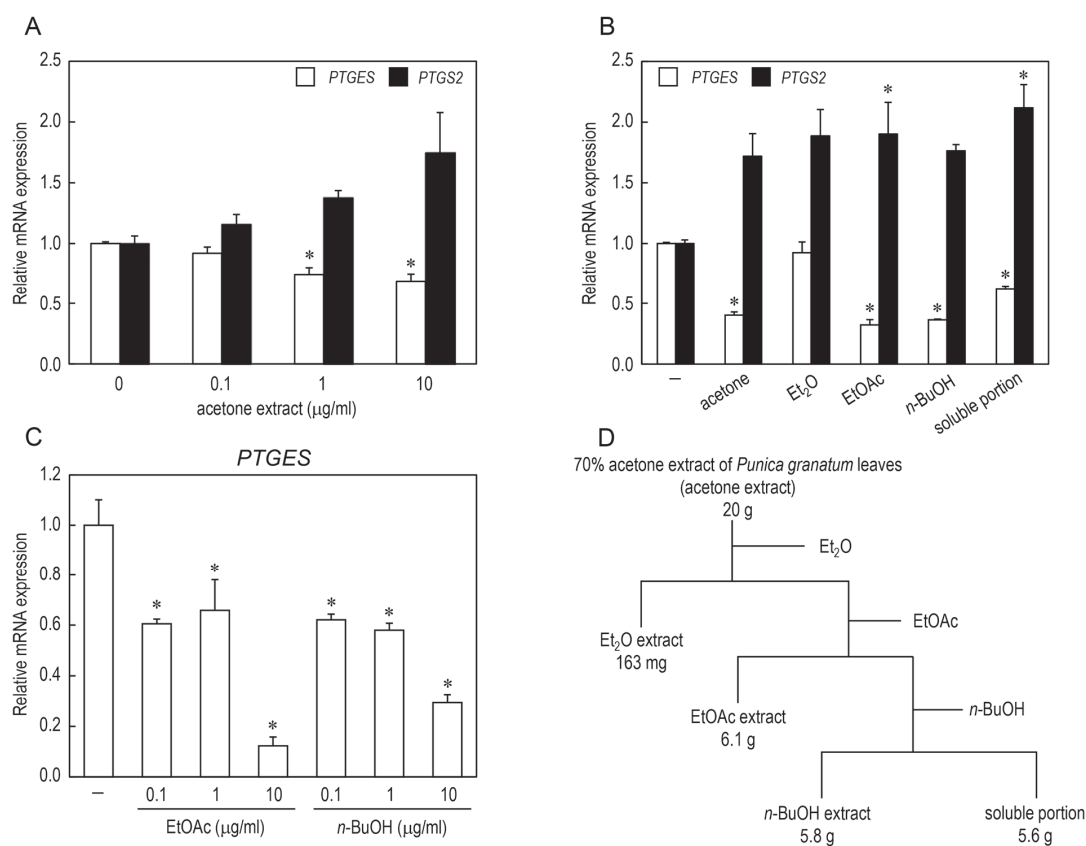


**Fig. 3. Effect of pomegranate leaf extract on the mRNA expression of *PTGES* (mPGES-1) and *PTGS2* (COX-2) in A549 cells.**

Changes in mRNA levels of *PTGES* (open bar) and *PTGS2* (closed bar) by treatment with acetone extract (0–10 µg/ml, A); each extract from pomegranate leaf (10 µg/ml, B), and EtOAc and *n*-BuOH extracts (C) was analyzed by real-time PCR, as described in the Materials and Methods section. The scheme of extraction and fractionation from *Punica granatum* leaves is shown in D. The values are represented as a relative value against control without extract treatment and represent mean ± SEM ( $n = 4$ ; A, B,  $n = 3$ ; C). \* $p < 0.01$ , compared with control without extract treatment.

ellagitannins granatin A and granatin B (Fig. 4) were identified as major components in the EtOAc and *n*-BuOH fractions<sup>24–26</sup>. Their structural analog geraniin is known as being a main polyphenolic component of *Geranium thunbergii*, a medicinal plant with an antidiarrheic effect<sup>27,28</sup>. These ellagitannins contain a dehydrohexahydroxydiphenoyl (DHHDP) group, which has been reported to have anti-inflammatory effects<sup>29,30</sup>. Therefore, these ellagitannins were listed as candidate ingredients to suppress mPGES-1.



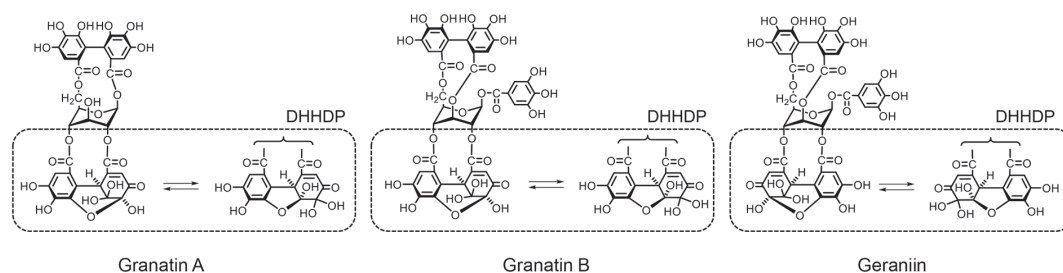


**Fig. 4. Chemical structure of granatin A, granatin B, and geraniin.**

The abundant compounds in EtOAc and *n*-BuOH extracts were identified as granatin A and granatin B. Chemical structures of the ellagitannins and their structural analog geraniin are shown. The dashed lines indicate the DHHDP group.

Granatin A, granatin B, and geraniin suppressed the mRNA expression of mPGES-1 in a dose-dependent manner (Fig. 5A). Treatment with 10  $\mu$ M granatin A, granatin B, and geraniin decreased mRNA levels of mPGES-1 significantly, to 23%, 15%, and 33%, respectively, compared to the control without treatment, whereas they did not affect those of COX-2 (Fig. 5A). Granatin A, granatin B, and geraniin also suppressed the expression of mPGES-1 protein (Fig. 5B), and reduced the ratio of mPGES-1 against COX-2 to 75%, 53%, and 65%, respectively, compared to control without treatment (IL-1 $\beta$ +/-vehicle in Fig. 5B). In particular, granatin B reduced the ratio by less than the level of control cells without IL-1 $\beta$  stimulation (IL-1 $\beta$ -/-vehicle in Fig. 5B). IL-1 $\beta$  stimulation increased the mPGES-1 activity of the microsomal fraction in A549 cells approximately 4-fold ( $200 \text{ nmol} \cdot \text{min}^{-1} \cdot \text{mg}^{-1}$ ) (Fig. 5C), and 24 h treatments with 10  $\mu$ M of granatin A, granatin B, and geraniin decreased the activity to 17%, 16%, and 11%, respectively, which activities were lower than the activity without IL-1 $\beta$  stimulation. It was also confirmed that IL-1 $\beta$  stimulation in the culture medium of A549 cells increased PGE<sub>2</sub> release to approximately 12-fold ( $5 \text{ ng} \cdot 1 \times 10^4 \text{ cells}^{-1}$ ) and that pretreatment with 10  $\mu$ M of granatin A, granatin B, and geraniin decreased PGE<sub>2</sub> release significantly, to 65%, 45%,

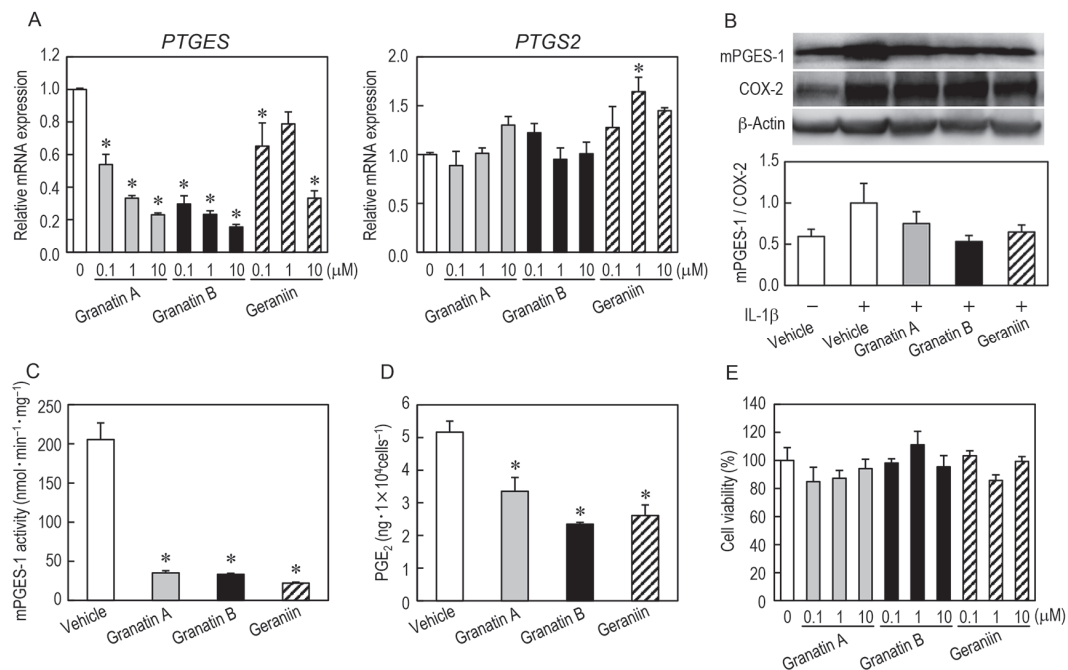


**Fig. 5. Effects of granatin A, granatin B, and geraniin on mPGES-1 and COX-2 expression.** Real-time PCR (A) and western blotting (B) were used to measure mRNA and protein expression of *PTGES* (mPGES-1) and *PTGS2* (COX-2), respectively. The mPGES-1 protein band density was corrected with COX-2; the ratio is represented as a relative value against the IL-1β (+) control in 6 separate analyses (lower graph in B). mPGES-1 activity after treatment with either granatin A, granatin B, or geraniin (10 μM) was measured, as described in the Materials and Methods section (C). PGE<sub>2</sub> released in the culture medium of A549 cells was quantified by enzyme immunoassay (D). Cell viability was assessed after 24 h using the CellTiter-Glo® 2.0 Assay (E). The values are represented as a relative value against control cells and represent mean ± SEM ( $n = 4$ ; A, C, E,  $n = 3$ ; D,  $n = 6$ ; B). \* $p < 0.01$ , compared with control without treatment with ellagitannins.

and 50%, respectively (Fig. 5D). To exclude the possibility that the cytotoxic action of granatin A, granatin B, and geraniin was responsible for suppressing gene expression, it was examined the effect of these ellagitannins on cell viability. Under the experimental conditions described above, there was no significant change in cell viability (Fig. 5E).

Inflammation-related genes, tumor necrosis factor  $\alpha$  (TNF $\alpha$ ), and iNOS, were down-regulated in a dose-dependent manner by the addition of granatin A, granatin B, and geraniin, excluding the expression of TNF $\alpha$  at 10 μM geraniin (Fig. 6A). Further, the ellagitannins suppressed anti-apoptotic factor Bcl-2 markedly in a dose-dependent

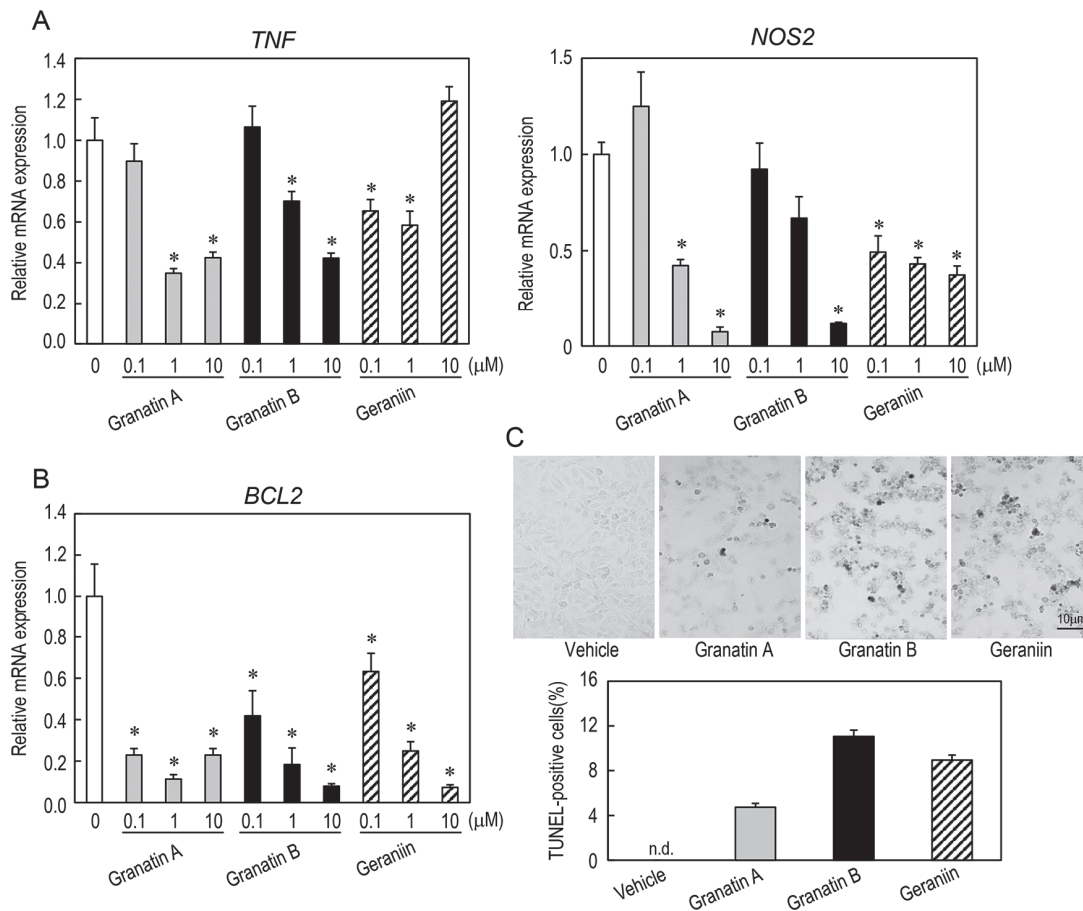


**Fig. 6. Changes in mRNA expression of *TNF* ( $TNF\alpha$ ), *NOS2* (iNOS) (A) and *BCL2* (Bcl-2) (B), and *in situ* detection of apoptotic cells (C) after treatment with granatin A (shaded bar), granatin B (closed bar), and geraniin (hatched bar).**

The values are represented as a relative value against control cells, and they represent mean  $\pm$  SEM ( $n = 4$ ; A, B). \* $p < 0.01$ , compared with control without treatment with ellagitannins. *In situ* apoptotic cells were detected by the TUNEL method, as described in the Materials and Methods section. The scale bar indicates 10  $\mu$ m.

manner (Fig. 6B). Treatment with granatin A, granatin B, or geraniin for 48 h increased *in situ* apoptotic positive cells with the TUNEL method, and the percentage of positive cells was high in granatin B, geraniin, and granatin A, in that order; however, this was hardly observed in the control cells (Fig. 6C). In lung carcinoma A549 cells, it has been reported decrease in  $PGE_2$  production leads cells to apoptosis and anti-inflammation<sup>11,31</sup>; thus, our finding suggests that the apoptosis of the A549 cells was due to suppression of mPGES-1 by the ellagitannins. These findings are consistent with previous reports that

granatin B <sup>32</sup> and geraniin <sup>33</sup> induce cancer cell apoptosis and have anti-cancer activity, and our present study added more information on the mechanism of involvement of ellagitannins in the regulation of mPGES-1.

## DISCUSSION

The mechanisms of multiple signal transduction regulate pro-inflammation and carcinogenesis. TNF $\alpha$  is a well-known inflammatory cytokine with pleiotropic actions in tumorigenesis, inflammation, and other disorders through specific cell surface receptors; therefore, it is a potent therapeutic target, and anti-TNF agents have, in fact, been approved <sup>34</sup>. The present findings showed that ellagitannins with the DHHD group suppressed TNF $\alpha$  expression, suggesting that they are anti-inflammatory. Nuclear factor- $\kappa$ B (NF- $\kappa$ B) acting downstream of TNF receptors and toll-like receptors is a potent transcriptional factor of COX-2 and iNOS. The COX-2 promoter not only has an NF- $\kappa$ B site but also an CCAAT/enhancer-binding protein (C/EBP) site, cAMP response element-1 (CRE-1), E-box, and AP-1 as transcriptional response elements, and these elements are conserved across different species <sup>35,36</sup>. On the other hand, the mPGES-1 promoter does not have binding sites for NF- $\kappa$ B and CRE contributing to COX-2 induction, suggesting that the inducible mechanism of mPGES-1 is distinct from that of COX-2 <sup>37</sup>. In this study, the ellagitannins down-regulated mPGES-1 and iNOS but not COX-2. This suggests that the ellagitannins have diverse influences on the different signals instead of NF- $\kappa$ B, and, thus, may down-regulate TNF $\alpha$ , iNOS, and mPGES-1 without side effects by COX-2 blockage. C. Lee *et al.* reported that granatin B reduces PGE<sub>2</sub> production by suppressing the expression of COX-2 protein in LPS-stimulated RAW264.7 cells <sup>30</sup>; their findings are different from our data. One reason for this may be related either to the CRE-2 element being found in mice but not in humans <sup>35,36</sup>, or the possibility that the ellagitannins have the other indirect regulation to COX-2 expression. C. Lee *et al.* did not study the effects

on mPGES-1 expression, and so this is the first report that the ellagitannins, including granatin B, down-regulated mPGES-1 expression and decreased PGE<sub>2</sub> production.

Curcumin <sup>38</sup>, diosgenin <sup>12</sup>, sulforaphane <sup>39</sup>, and sinomenine <sup>40</sup> have been reported to suppress the expression of mPGES-1, although there have been only a few reports of phytochemicals down-regulating mPGES-1. Curcumin and diosgenin affect not only mPGES-1 but also COX-2, and several phytochemicals down-regulating COX-2 have been reported <sup>41</sup>. Granatin A, granatin B, and geranin suppressed mPGES-1 expression more strongly than established phytochemicals such as sulforaphane and sinomenine. These ellagitannins can be expected to be both efficacious and safe, without the side effects caused by COX inhibition.

In conclusion, it is suggested that part of the mechanism of anti-inflammatory and anti-tumor effects by DHHDP group-containing ellagitannins, including granatin A, granatin B, and geraniin, is through down-regulation of mPGES-1, suggesting that the ellagitannins have novel functionality. It can be expected that they can be used to prevent and treat several inflammatory disorders without side effects, unlike the cases of existing NSAIDs that target COX. There is need of *in vivo* studies using inflammatory model animals to confirm the biological effects.

## **Chapter III**

**Red-kerneled rice proanthocyanidin inhibits  
arachidonate 5-lipoxygenase and decreases  
psoriasis-like skin inflammation**

Colored rice contains a lot of polyphenols such as anthocyanin and proanthocyanidin <sup>42</sup>. N. Ganeko *et al.* recently isolated and identified a proanthocyanidin from the hulls of red-kerneled rice (red-kerneled rice proanthocyanidin; RRP) <sup>43</sup>. RRP is an octamer of catechin with an average molecular weight 2338. Red-kerneled rice is reported to have potent antioxidant <sup>44</sup> and anti-inflammatory activities <sup>45</sup>. In the present study, the mechanism of RRP on 5-LOX and/or LTB<sub>4</sub>-related inflammation was investigated, and confirmed the effect in chronic skin inflammation model mice.

Psoriasis is a classic type 1 autoimmune disease characterized by chronic skin inflammation with scaly erythematous plaques and marked epidermal hyperplasia <sup>46</sup>. In the pathogenesis of psoriasis, IL-23 facilitates IL-17 production from T helper 17 (Th17) cells, leading to epidermal hyperplasia and inflammatory cell infiltration <sup>46,47</sup>. In psoriatic skin lesions, neutrophils infiltrate the dermis during the early phase <sup>48</sup>, and LTB<sub>4</sub> production increases <sup>49</sup>. LTB<sub>4</sub> plays a role in neutrophil recruitment through the receptor BLT1, which is coordinated with CXCR2, a chemokine receptor for CXCL 1/2, in imiquimod (IMQ)-induced psoriasis-like skin in mice <sup>50,51</sup>. Therefore, 5-LOX inhibitors may be useful therapeutic agents for psoriasis.

In this chapter, it is reported that RRP inhibits 5-LOX, catalyzing the first process to produce LTA<sub>4</sub> as a precursor of several LTs, and improves IMQ-induced psoriasis-like skin as a chronic inflammation <sup>52</sup>.



## MATERIALS AND METHODS

### *Preparation of proanthocyanidin derived from red-kerneled rice*

Red-kerneled rice proanthocyanidin was prepared as described previously <sup>43</sup>. The rice hulls from red-kerneled rice (*Oryza sativa*, Red rice company Co., Ltd. Soja, Japan) were homogenized with 70% aqueous acetone, and the crude extract was loaded onto a column packed with Diaion HP-20 resin. A polyphenol-rich fraction was isolated with 50% methanol. Gel permeation chromatography analysis confirmed the presence of the RRP catechin octamer (Fig. 7) in this fraction based on its molecular weight. The dried RRP was redissolved in 50% ethanol or DMSO for *in vivo* or *in vitro* study, respectively.

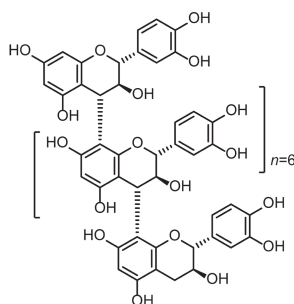


**Fig. 7. Chemical structure of RRP.**

### *Cell culture and treatment*

Rat basophilic leukemia cell line RBL-2H3 (Japanese Cancer Research Resources Bank, Tokyo, Japan), human non-small-cell lung carcinoma cell line A549 (ATCC CCL-185), and human embryonic kidney (HEK) 293T cell (RIKEN BioResource Center, Tsukuba, Japan) were cultured in Roswell Park Memorial Institute medium and

DMEM containing 10% fetal bovine serum, 100 units/mL penicillin, and 100 µg/mL streptomycin. The cells were maintained at 37°C in a humidified atmosphere of 95% air and 5% CO<sub>2</sub>. RBL-2H3 and A549 cells were incubated for 16 h with 0–10 µM RRP in DMSO or vehicle only as a control. Cell viability was measured using CellTiter-Glo 2.0 Assay (Promega, Madison, WI, USA).

### ***Enzyme immunoassay***

Arachidonic acid (10 µM) and A-23187 (5 µM) were added to the RBL-2H3 cell culture medium to induce LTB<sub>4</sub> synthesis, and arachidonic acid (10 µM) was added to the culture medium of A549 cells to induce PGE<sub>2</sub> synthesis. After incubation for 5 min or 30 min, the concentration of LTB<sub>4</sub> or PGE<sub>2</sub> in the medium was measured by enzyme immunoassay using the LTB<sub>4</sub> or PGE<sub>2</sub> ELISA Kit (Cayman Chemical Co. Ann Arbor, MI, USA) according to the manufacturer's instructions.

### ***LOX and COX assays***

The enzyme activity of 5-LOX, leukocyte-type 12-LOX, COX-1, and COX-2 was assayed as described previously<sup>53,54</sup>. 5-LOX<sup>55</sup>, 12-LOX<sup>56</sup>, COX-1<sup>57</sup>, and COX-2<sup>57</sup> were partially purified from RBL-2H3 cells, J774A.1 cells overexpressing porcine 12-LOX, and COLO320DM cells overexpressing COX-1 and COX-2, respectively. Human recombinant 5-LOX was purchased from Cayman Chemical. These enzymes were preincubated for 5 min at 4°C with or without RRP and catechin (Sigma-Aldrich, St. Louis, MO, USA) and the enzyme reaction started by the addition of 25 µM arachidonic acid for 5-LOX and 12-LOX or 25 µM linoleic acid for COX under optimum reaction conditions. The LOX reactions were carried out in the following buffers: 5-LOX, 100

mM Tris-HCl (pH 7.4), 2 mM CaCl<sub>2</sub>, and 2 mM adenosine triphosphate (5 min at 30°C); 12-LOX, 100 mM Tris-HCl (pH 7.4) (5 min at 30°C). The products were reduced by the addition of glutathione peroxidase (0.1 unit) and 5 mM glutathione, followed by incubation for a further 20 min. COX-1 and COX-2 were assayed in 100 mM Tris-HCl (pH 7.4), 2 μM hematin, and 5 mM tryptophan for 5 min at 24°C. After acidification of the reaction mixture by the addition of 100 mM HCl, 0.25 nmol of 15-hydroxyeicosadienoic acid was added as an internal standard. The products were analyzed by RP-HPLC using a COSMOSIL 5C18-MS-II column (5 μm particle, 4.6 × 250 mm, Nacalai Tesque, Kyoto, Japan) with a solvent system of methanol/water/acetic acid (80:20:0.01, v/v). Absorption at 235 nm was continuously monitored using a Waters 2489 UV/Visible detector. The metabolites, 5-hydroxyeicosatetraenoic acid (HETE) in the 5-LOX reaction, 12- and 15-HETE in the leukocyte-type 12-LOX reaction, and 9- and 13-hydroxyoctadecadienoic acid in the COX reaction, were quantified by comparing the area under the peak with that of an internal standard. To determine whether RRP chelates calcium ions, EDTA was used as a positive control.

### ***PGES assay***

Recombinant human mPGES-1 was used for the PGES assay. HEK293T cells were transfected with the expression vector pCMV6-Entry-PTGES (Origene Technologies, Inc., Rockville, MD, USA) using Lipofectamine 2000 (Life Technologies, Carlsbad, CA, USA) according to the manufacturer's instructions. After 2 days, the cells were scraped off the dishes and disrupted by sonication in 10 mM potassium phosphate buffer (KPB), pH 7.2, and the microsome fraction was used as the enzyme source. Membrane-bound PGES-2 (mPGES-2) and cytosolic PGES (cPGES) were prepared from

the microsomal and cytosolic fractions of A549, respectively. Fraction samples were preincubated for 15 min at 4°C with or without RRP and catechin, and mPGES-1 activity was initiated by the addition of 80  $\mu$ M PGH<sub>2</sub> in 100 mM KPB (pH 7.2) with 2.5 mM glutathione and incubated for 1 min at 24°C. mPGES-2 activity was initiated by the addition of 40  $\mu$ M PGH<sub>2</sub> in 100 mM KPB (pH 6.5) with 1 mM DTT and incubated for 1 min at 24°C. cPGES activity was initiated by the addition of 100  $\mu$ M PGH<sub>2</sub> in 100 mM Tris–HCl buffer (pH 8.0) with 2.5 mM glutathione and incubated for 1 min at 24°C. The reaction was terminated using 100 mM FeCl<sub>2</sub>/0.5 M citric acid, and 2.5 nmol of PGB<sub>2</sub> was added as an internal standard. The produced PGE<sub>2</sub> was analyzed as described above using a solvent system of ACN/water/acetic acid (40:60:0.01, v/v). Absorption at 192 nm was continuously monitored.

### ***Psoriasis-like mouse model***

Seven-week-old male BALB/c mice (24–28 g) were purchased from Charles River Laboratories, Inc. (Wilmington, MA, USA). Mice were housed under specific pathogen-free conditions and had free access to drinking water and food (CRF-1, Oriental Yeast Co., Ltd., Tokyo, Japan). Each experimental group had 6 mice. Psoriasis-like mouse skin was induced as described previously<sup>52</sup>. In brief, 12.5 mg IMQ cream (Beselna cream 5%, Mochida Pharmaceutical Co., Ltd., Tokyo, Japan) was applied to the ear for 5 consecutive days (total, 62.5 mg IMQ/mouse). On day 6, the ear thickness was measured with a Quick Micro (Mitutoyo Co., Kanagawa, Japan), and the mice were sacrificed. All protocols were approved by the Exclusive Committee on Animal Research at Okayama Prefectural University, and the study was conducted in accordance with the Public Health Service policy.

### ***Dosage information/Dosage regimen***

RRP (50  $\mu$ L/ear/day containing 25, 250, or 2500  $\mu$ g; 0.2, 2, or 20 mM/ear/day, i.e., 2, 20, or 200 mg/kg/day) was applied topically to the ear of each mouse 30 min before the application of IMQ cream for 5 days. These doses are equivalent to human at 0.16, 1.62, and 16.2 mg/kg/day converted to take into account the body surface area <sup>58</sup>. The dose of RRP was determined according to information in another report <sup>59</sup>. Throughout the experiment, RRP-treated mice presented with no abnormalities and had no significant changes in weight or food intake as compared to control mice.

### ***Histopathological and immunohistochemical analyses***

For histological analysis, IMQ-induced mouse ears treated with RRP or vehicle were fixed in 100 mM sodium phosphate buffer (pH 7.4) containing 4% (w/v) paraformaldehyde and embedded in paraffin. The sections were used for hematoxylin and eosin (HE) staining and observed by light microscopy. Changes in spinous layer thickness were measured under the microscope.

For immunohistochemical analysis, the fixed ears were embedded in Tissue-Tek OCT compound (Sakura Finetek Japan Co., Ltd., Tokyo, Japan). The sectioned tissues were treated with 3% hydrogen peroxide to block endogenous peroxidase activity and 10% Block Ace (DS Pharma Biomedical Co., Ltd., Tokyo, Japan) to block nonspecific binding. For immunolabeling neutrophils, the primary antibody was rat anti-Ly-6G/Ly-6C (Gr-1) antibody (1:200; catalog no. 108413, lot no. B141536, BioLegend, San Diego, CA), and the secondary antibody was FITC-labeled donkey anti-rat IgG (1:400, Jackson ImmunoResearch Laboratories, Inc., West Grove, PA. USA). The sections were mounted using Vectashield mounting medium for fluorescence with 4',6-diamidino-2-phenylindole

(DAPI, Vector Laboratories, Inc., Burlingame, CA, USA) and observed by confocal laser scanning light microscopy (Fluoview FV1000, Olympus Co., Tokyo, Japan).

### ***Real-time quantitative PCR***

Total RNA was isolated using the RNeasy plus Mini Kit (Qiagen N.V., Hilden, Germany), and cDNA was prepared using High-Capacity cDNA Reverse Transcription Kit (Applied Biosystems, LLC, Foster City, CA, USA). Quantitative PCR was performed using SsoAdvanced Universal SYBR Green Supermix (Bio Rad Labs., Hercules, CA, USA) on the StepOnePlus Real-Time PCR System (Applied Biosystems, LLC, Foster City, CA, USA), and the following primer pairs: *Alox5*, 5'-AGCGGCAGCTCAGTTAGAA-3' (forward) and 5'-GGAAGTGGTGTGTACAGGGG-3' (reverse); *Il17a* (IL-17A), 5'-CAGGGAGAGCTTCATCTGTGT-3' (forward) and 5'-GCTGAGCTTTGAGGGATGAT-3' (reverse); *Il22* (IL-22), 5'-CGTCAACCGCACCTTTAT-3' (forward) and 5'-AGGGCTGGAACCTGTCTG-3' (reverse); *S100a9* (S100a9), 5'-GACACCCTGACACCCTGAG-3' (forward) and 5'-TGAGGGCTTCATTTCTCTTCTC-3' (reverse); *Krt1* (keratin 1), 5'-TTTGCCTCCTTCATCGACA-3' (forward) and 5'-GTTTTGGGTCCGGGTTGT-3' (reverse); *Gapdh* (GAPDH), 5'-TGTTCCCTACCCCCAATGTGT-3' (forward) and 5'-CCCTGTTGCTGTAGCCGTAT-3' (reverse). Data were normalized to *Gapdh* expression level.

### ***Electrospray ionization mass spectrometry (ESI-MS)***

Samples were prepared as described previously<sup>60</sup>. Mouse ears were homogenized using a Polytron homogenizer in 2 mL of ice-cold methanol and incubated at -30°C overnight. The lipid components were extracted using the Bligh and Dyer method<sup>61</sup>, and

the recovery of each lipid throughout the procedure was calibrated against an internal added standard of 500 pmol *d4*-labeled PGE<sub>2</sub> or *d5*-labeled eicosapentaenoic acid. For analysis of the fatty acid metabolites LT and PG, lipids were extracted using Oasis HLB cartridges (Waters, Milford, MA, USA) and were dried under nitrogen gas. The analysis was performed using a 4000Q-TRAP quadrupole-linear ion trap hybrid mass spectrometer (AB Sciex, Framingham, MA, USA) with LC (NexeraX2 system; Shimadzu Co., Kyoto, Japan). The sample was applied to a C18 column (Kinetex C18, 2.1 × 150 mm, 1.7 μm, Phenomenex, Inc., Torrance, CA, USA) coupled for ESI-MS/MS. For fatty acid analysis, the samples were applied to a column and separated using a step gradient with mobile phase A (ACN:methanol:water, 1:1:1 (v/v/v) containing 5 μM phosphoric acid and 1 mM ammonium formate) and mobile phase B (2-propanol containing 5 μM phosphoric acid and 1 mM ammonium formate) at a flow rate of 0.2 mL/min at 50°C. To analyze oxidized fatty acids, the samples are applied to a column and separated using a step gradient with mobile phase C (water containing 0.1% acetic acid) and mobile phase D (ACN:methanol, 4:1; v/v) at a flow rate of 0.2 mL/min at 45°C. Signature ion fragments for each target lipid were monitored and quantified by multiple reaction monitoring (MRM). Lipids were identified by the MRM transition<sup>62</sup> and retention times based on the peak area of the MRM transition and the calibration curve for an authentic standard for each compound.

### ***Statistics***

Data were analyzed using Student's *t*-test and Dunnett's post-hoc test at a significance level of  $p < 0.01$ .

## RESULTS

### *Inhibitory effect of RRP on lipoxygenase and cyclooxygenase activity*

RRP inhibited rat 5-LOX and porcine leukocyte-type 12-LOX activity dose-dependently, with  $IC_{50}$  values of 7.0  $\mu$ M and 47.5  $\mu$ M, respectively (Fig. 8A). RRP up to 500  $\mu$ M had no effect on COX-1 or COX-2 activity, whereas catechin monomer inhibited rat 5-LOX and COX-1 activity ( $IC_{50}$ , 9.0 and 30.0  $\mu$ M, respectively) (Fig. 8D). RRP and catechin also inhibited human 5-LOX ( $IC_{50}$ , 16.8 and 2.0  $\mu$ M, respectively) (data not shown). Michaelis–Menten kinetics (Fig. 8B, E) and Lineweaver–Burk plot analysis (Fig. 8C, F) of 5-LOX with RRP or catechin, and the changes in  $K_m$  and  $V_{max}$  values for 5-LOX are shown in Table 1. The data demonstrate that RRP and catechin increased the  $K_m$  and

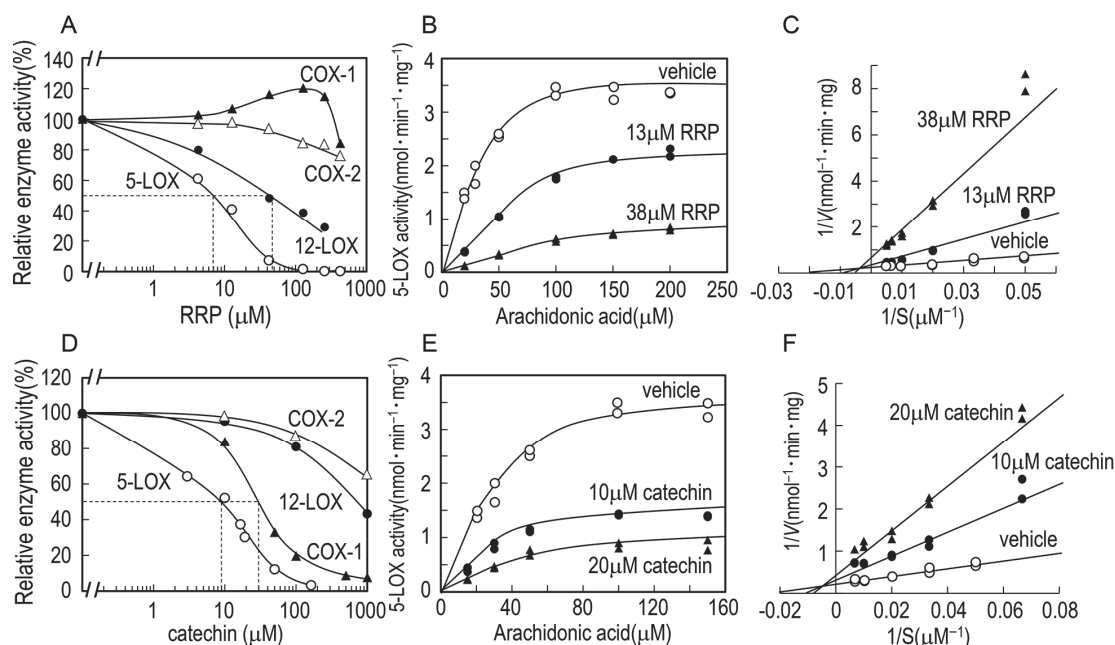


**Fig. 8. Effect of RRP (A–C) and catechin (D–F) on 5-LOX, 12-LOX, COX-1, and COX-2 activity.**

5-LOX and 12-LOX were incubated with 25  $\mu$ M arachidonic acid at 30°C for 5 min, and COX-1 and COX-2 were incubated with 25  $\mu$ M linoleic acid at 24°C for 5 min with RRP (A) or catechin (D). Inhibitory effects on the enzymes by RRP or catechin (A and D), and Michaelis–Menten plot (B and E) and Lineweaver–Burk plot (C and F) with or without RRP or catechin are shown.



**Table 1.**  $K_m$  and  $V_{max}$  values calculated based on Lineweaver–Burk plot against 5-LOX (Fig. 8C, F)

Inhibitor ( $\mu\text{M}$ )		$K_m$ ( $\mu\text{M}$ )	$V_{max}$ ( $\text{nmol} \cdot \text{min}^{-1} \cdot \text{mg}^{-1}$ )
vehicle		47.6	4.4
RRP	13	111.1	3.1
	38	200.0	1.6
catechin	10	79.7	2.7
	20	118.5	2.1

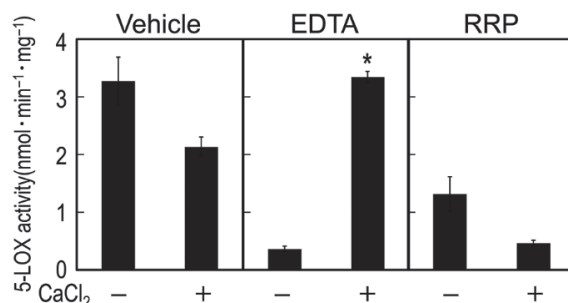


**Fig. 9. Investigation of calcium ion chelate effect.**

5-LOX preincubated with (+) or without (–) 200  $\mu\text{M}$   $\text{CaCl}_2$  was incubated with 25  $\mu\text{M}$  arachidonic acid at 30°C for 5 min, in the reaction mixture (100 mM Tris–HCl (pH 7.4), 400  $\mu\text{M}$   $\text{CaCl}_2$ , and 2 mM adenosine triphosphate) in the presence of Vehicle (1% DMSO) or 10  $\mu\text{M}$  RRP or 200  $\mu\text{M}$  EDTA and the products were quantified using RP–HPLC ( $n=3$ ). The values represent mean  $\pm$  SEM. \* $p < 0.01$  compared with treatment with EDTA  $\text{CaCl}_2$  (–).

decreased the  $V_{max}$  of 5-LOX activity, indicating that RRP and catechin are mixed noncompetitive inhibitors of 5-LOX. Calcium ion is required for 5-LOX activity *in vitro*<sup>63,64</sup> and is also essential for translocation of 5-LOX from the cytoplasm to the membrane in leukocytes<sup>65</sup>. As shown in Fig. 9, the specific activity of 5-LOX was reduced by approximately 90% by the addition of EDTA as a calcium ion chelating agent and was then restored to the original specific activity by the addition of 200  $\mu\text{M}$   $\text{CaCl}_2$ . In contrast, the RRP-induced decrease in 5-LOX activity was not restored by the addition of  $\text{CaCl}_2$ , suggesting that the mechanism of RRP inhibition of 5-LOX did not involve chelation.

### ***Inhibitory effect of RRP on prostaglandin E synthase***

RRP also dose-dependently inhibited mPGES-1 and cPGES activity, with  $IC_{50}$  values of 7.7  $\mu$ M and 45.3  $\mu$ M, respectively (Fig. 10A). However, RRP up to 500  $\mu$ M had no effect on mPGES-2 activity, and catechin monomer (up to 200  $\mu$ M) had no effect on mPGES-1 (Fig. 10D). Michaelis–Menten kinetics and Lineweaver–Burk plot analysis of mPGES-1 with RRP (Fig. 10B, C) and the  $K_m$  and  $V_{max}$  values of mPGES-1 are shown in Table 2. The data show that RRP did not affect the  $K_m$  but decreased  $V_{max}$  against mPGES-1 activity, indicating that RRP is a noncompetitive inhibitor of mPGES-1.

### ***RRP decreases LTB<sub>4</sub> and PGE<sub>2</sub> release from intact cells***

Pretreatment of RBL-2H3 and A549 cells with RRP dose-dependently decreased LTB<sub>4</sub> and PGE<sub>2</sub> production (Fig. 11A and C). To exclude the possibility of RRP cytotoxicity, it was investigated the effect of RRP on cell viability (Fig. 11B and D). Under the experimental conditions used to assess LTB<sub>4</sub> and PGE<sub>2</sub> production, cell viability was determined to be >90% (Fig. 11B and D).

### ***Morphological improvements in IMQ-induced skin inflammation by RRP***

The histological effects of RRP on IMQ-induced psoriasis-like skin were investigated. HE staining showed that IMQ-treated mouse ears had a thickened spinous layer and increased infiltration of inflammatory cells compared with normal controls (Fig. 12A). Topical application of RRP (25–2500  $\mu$ g/ear) dose-dependently suppressed the hyperplasia and decreased inflammatory cell infiltration. Immunohistochemical staining indicated that IMQ-treated mouse ears had more infiltrating neutrophils than did normal controls. The application of RRP (2500  $\mu$ g/ear) markedly decreased neutrophil infiltration

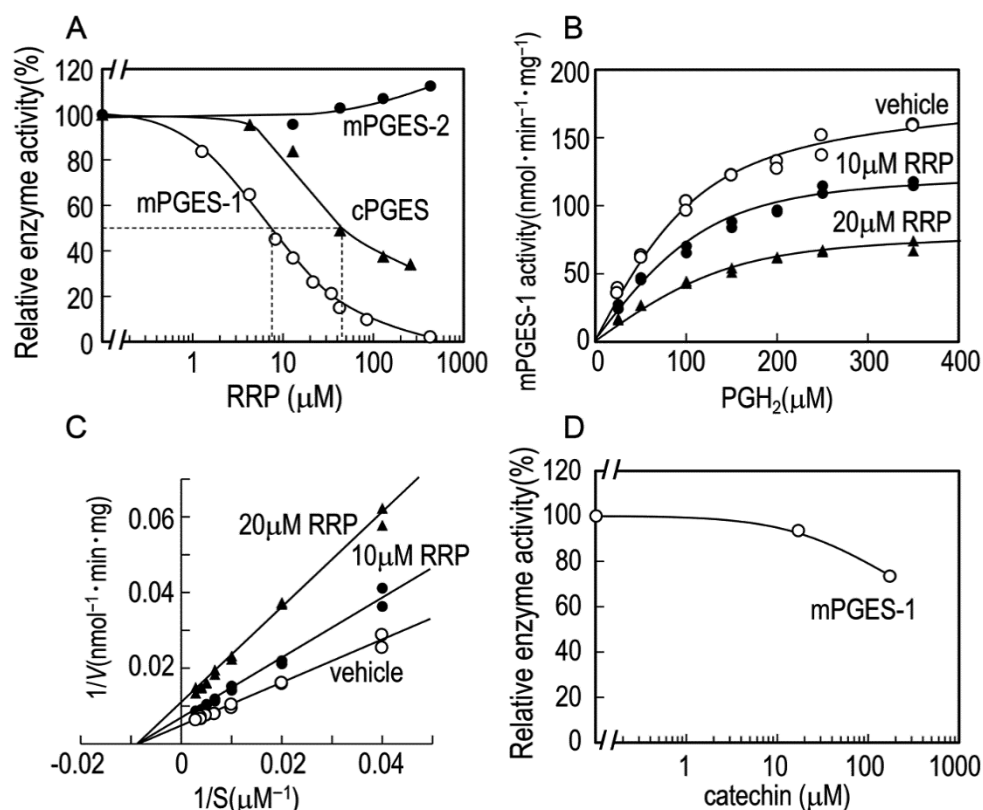


**Fig. 10. Effect of RRP and catechin on PGES activity.**

mPGES-1 and mPGES-2, cPGES were incubated with 80 and 40, 100  $\mu\text{M}$   $\text{PGH}_2$  at  $24^\circ\text{C}$  for 1 min in the presence of RRP (A), and mPGES-1 in the presence of catechin (D) at various concentrations and the products were quantified using RP-HPLC. Relative enzyme activities as compared with the activity without inhibitor are shown. Kinetic analysis of mPGES-1 inhibition by RRP was incubated with various concentrations of  $\text{PGH}_2$  at  $24^\circ\text{C}$  for 1 min in the absence of indicated concentrations of RRP. Michaelis–Menten plot (B) and Lineweaver–Burk plot (C) are shown.

**Table 2.**  $K_m$  and  $V_{\max}$  values calculated based on Lineweaver–Burk plot against mPGES-1

Inhibitor ( $\mu\text{M}$ )	$K_m$ ( $\mu\text{M}$ )	$V_{\max}$ ( $\text{nmol} \cdot \text{min}^{-1} \cdot \text{mg}^{-1}$ )
vehicle	125.0	217.4
RRP 10	125.0	156.3
RRP 20	125.0	95.2

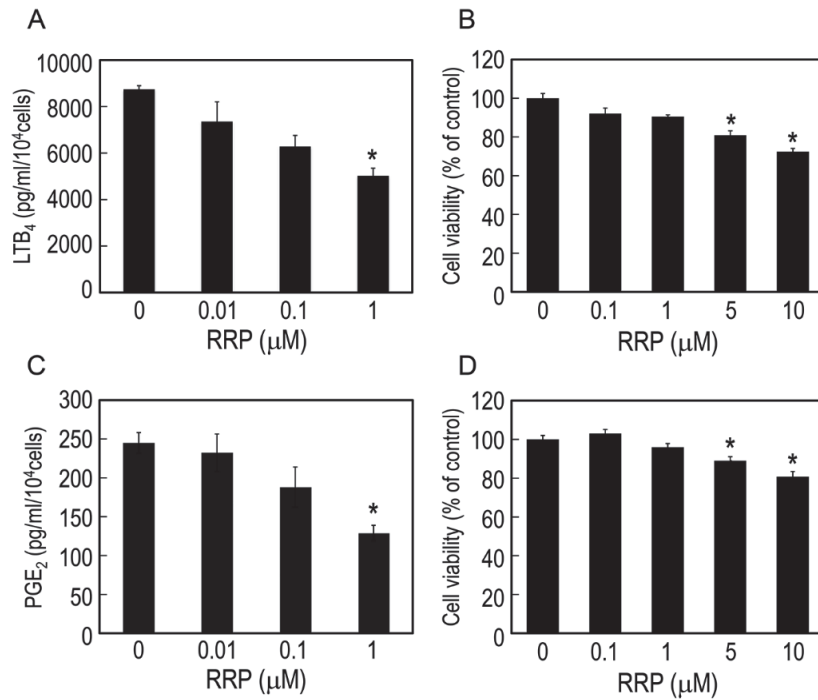


**Fig. 11. Effect of RRP on  $\text{LTB}_4$  or  $\text{PGE}_2$  production and cell viability in RBL-2H3 or A549.**  $\text{LTB}_4$  (A) and  $\text{PGE}_2$  (C) production were measured by ELISA ( $n=3$ ). Cells were treated with 0–10  $\mu\text{M}$  RRP, and viability was assessed after 16 h using CellTiter-Glo 2.0 Assay on RBL-2H3 (B) and A549 (D) cells ( $n=4$ ). The values represent mean  $\pm$  SEM. \* $p < 0.01$  compared with treatment with 0  $\mu\text{M}$  RRP.

(Fig. 12B). As shown in Fig. 12C, the ear thickness, as measured by micrometer, and spinous layer thickness, as measured by microscopy, significantly decreased to approximately 30% and 50%, respectively, of IMQ-treated ears after treatment with RRP (250 and 2500  $\mu\text{g}/\text{ear}$ ); the number of infiltrating neutrophils decreased significantly to about 10% of that of with IMQ-treated ears (Fig. 12C). Treatment with catechin monomer (0.1  $\mu\text{mol}$ ; corresponding to 250  $\mu\text{g}/\text{ear}$  RRP) resulted in no significant changes in ear thickness (Fig. 12C).

### ***Changes in psoriasis-associated mRNA expression in IMQ-induced mouse skin***

The expression of several psoriasis-related mRNAs in IMQ-induced mouse ears was investigated. The mRNA expression of *Alox5* (5-LOX), cytokines produced by Th17 cells *Il17a* (IL-17a) and *Il22* (IL-22), and markers of keratinocyte differentiation or activation *S100a9* (S100a9) and *Krt1* (Krt1) was analyzed by quantitative PCR (Fig. 13). *Il17a* and *Il22* mRNAs were markedly increased by IMQ treatment as compared to untreated mice (no expression). *S100a9* and *Krt1* increased approximately 5000-fold and 20-fold, respectively, compared with untreated mice. The IMQ-induced expression of *Il17a*, *Il22*, *S100a9*, and *Krt1* was dose-dependently suppressed by RRP. The expression of *Alox5* did not change with RRP treatment.

### ***Changes in eicosanoid production in IMQ-induced mouse skin***

The production of LTB<sub>4</sub>, 12-HETE, arachidonic acid, PGD<sub>2</sub>, PGE<sub>2</sub>, and PGF<sub>2α</sub> in mouse ears as determined by ESI-MS is shown in Fig. 14. The eicosanoids were increased by IMQ treatment. RRP treatment dose-dependently decreased LTB<sub>4</sub> in IMQ-induced mouse skin, reaching the level of LTB<sub>4</sub> production of normal mouse skin at a dose of 2500 µg/ear. In addition, 12-HETE production decreased significantly at a dose of 250 µg/ear RRP. In contrast, RRP treatment (2500 µg/ear) significantly increased PGD<sub>2</sub> and PGE<sub>2</sub> production. No significant differences were observed in the production of arachidonic acid or PGF<sub>2α</sub>, and the amounts of the other eicosanoids, including PGI<sub>2</sub>, thromboxane A<sub>2</sub>, and cysteinyl-LTs (LTC<sub>4</sub>, LTD<sub>4</sub>, and LTE<sub>4</sub>), were very low or undetectable.

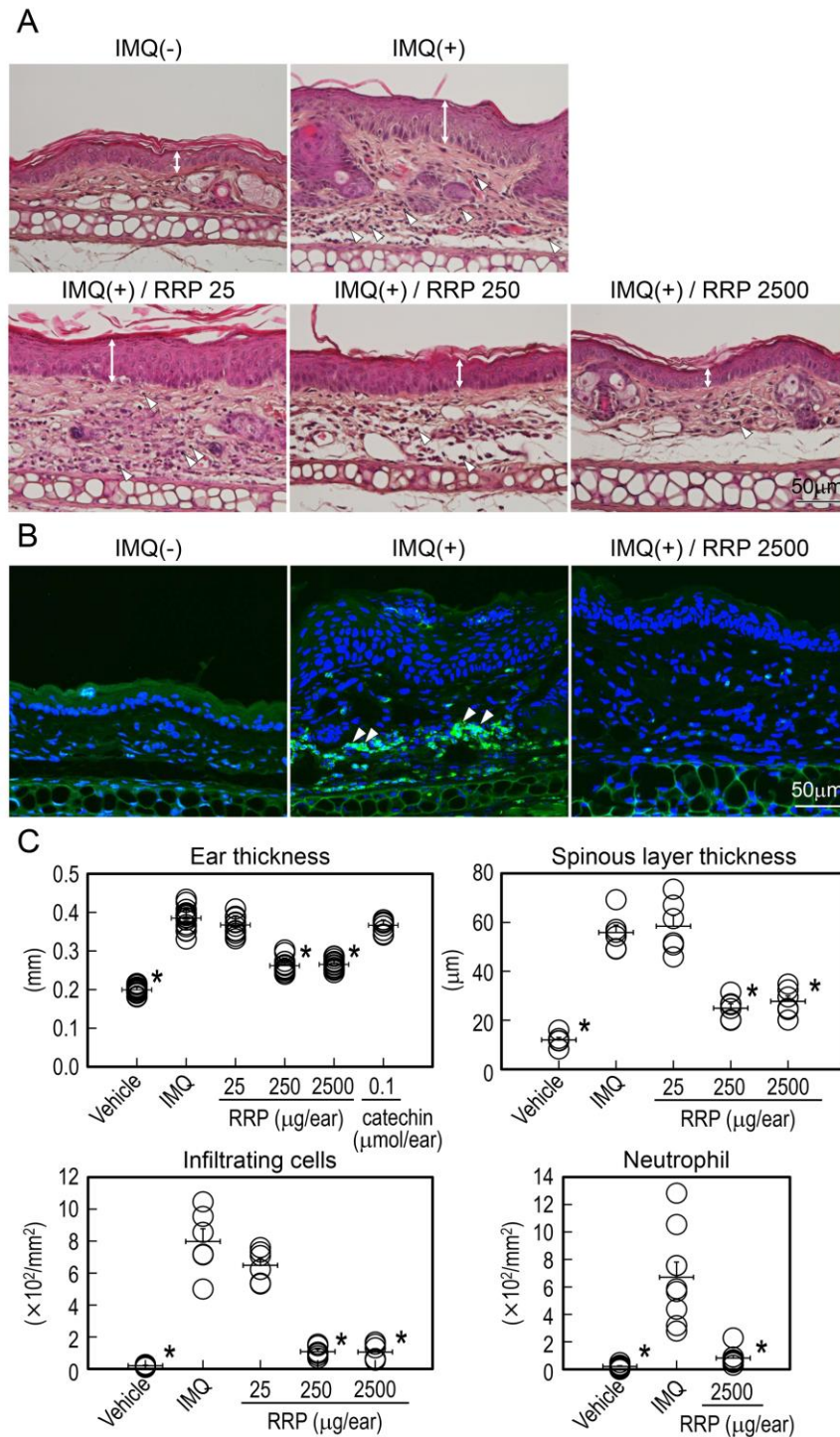


**Fig. 12. Histological and histochemical analyzes in mouse ear.**

Histological changes after RRP treatment were observed in HE staining (A) and immunofluorescent staining of Ly-6G/Ly-6C (green, Gr-1 as a neutrophil marker) and DAPI (blue, nuclear counterstain) (B). Ear thickness was measured by Quick Micro, and spinous layer thickness was measured under the microscope (upper graphs in C). Infiltrating cells and neutrophils were counted with HE staining and Ly-6G/Ly-6C immunofluorescent staining, respectively (lower graphs in C). *Double-headed arrows* indicate hyperplasia of stratum spinosum; *arrowheads* indicate infiltrating cells (A) and neutrophils (B). Data are presented as the mean  $\pm$  SEM. \* $p < 0.01$  vs. IMQ-induced control.

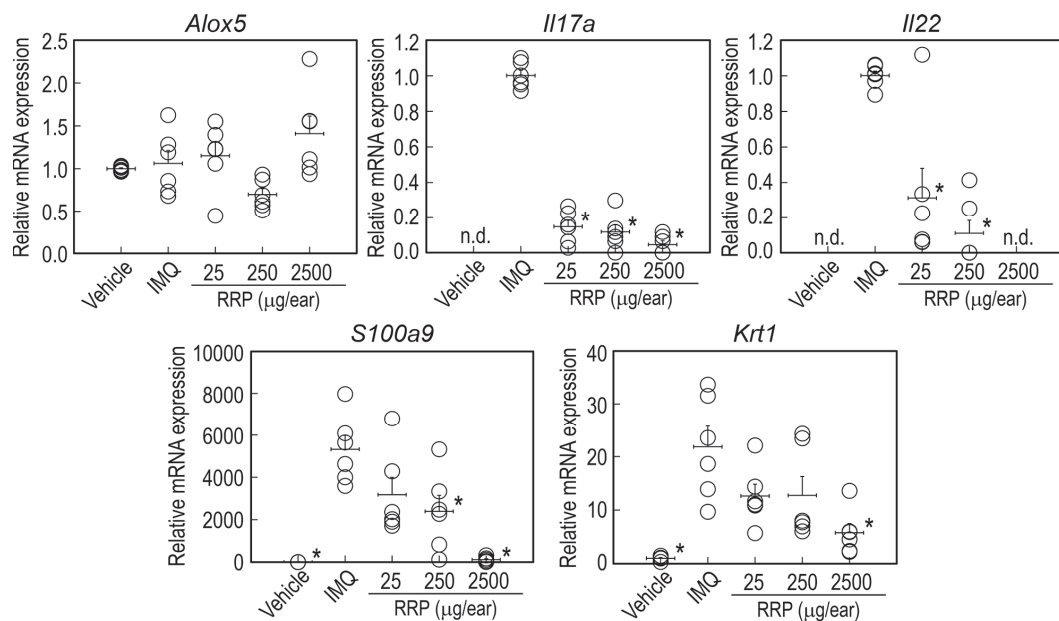


**Fig. 13. Changes in psoriasis-associated mRNA expression in IMQ-induced mouse skin.** Expression levels of *Alox5* (5-LOX), *Il17a* (IL-17a), *Il22* (IL-22), *S100a9* (S100a9), and *Krt1* (Krt1) were normalized to that of *Gapdh* (GAPDH). Relative expression of *Il17a* and *Il22* is shown vs. that of IMQ-treated mice; those of the other genes are shown vs. normal control. Data are presented as the mean  $\pm$  SEM of 6 mice per group. \* $p < 0.01$  compared with the IMQ-induced control. n.d., not detected.

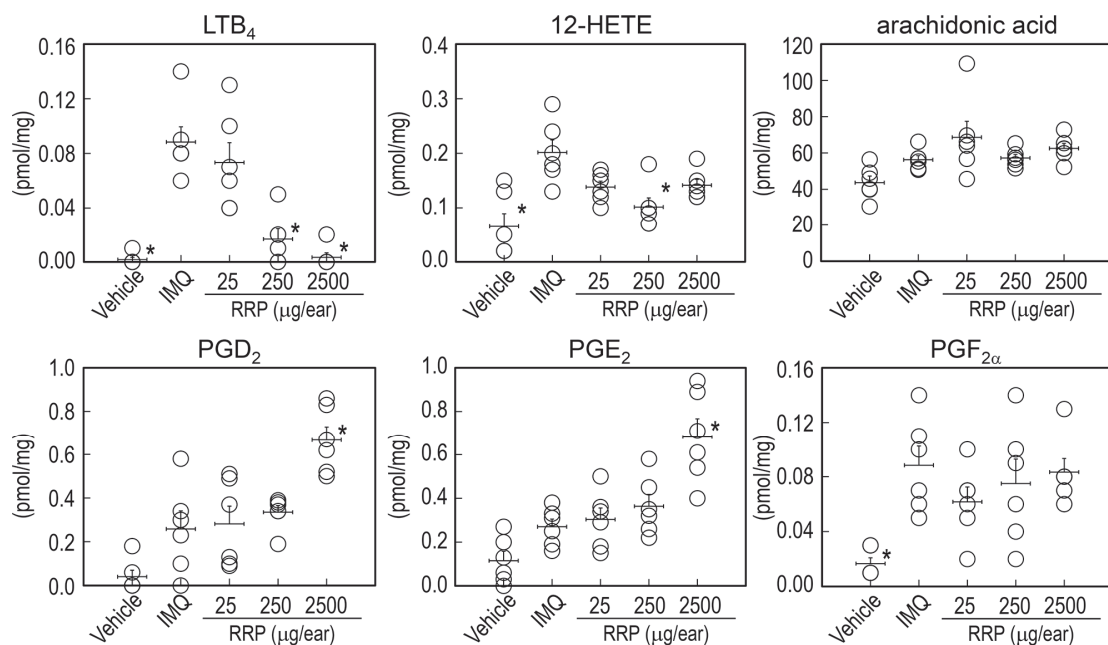


**Fig. 14. Changes in eicosanoid production.** The production of *LTB<sub>4</sub>*, 12-HETE, arachidonic acid, *PGD<sub>2</sub>*, *PGE<sub>2</sub>*, and *PGF<sub>2α</sub>* were analyzed by ESI-MS. Data are presented as the mean  $\pm$  SEM of 6 mice per group. \* $p < 0.01$  vs. IMQ-induced control.

## DISCUSSION

RRP exhibited potent mixed noncompetitive inhibition of 5-LOX, with an  $IC_{50}$  of 7.0  $\mu$ M. RRP decreased LTB<sub>4</sub> production in RBL-2H3 cells. Topical application of RRP to IMQ-induced psoriasis-like mouse skin suppressed hyperplasia, decreased inflammatory cell infiltration, down-regulated expression of the psoriasis-associated genes *Il17a*, *Il22*, *Sl00a9*, and *Krt1*, and decreased the production of LTB<sub>4</sub> but no other arachidonate metabolite.

In the pathogenesis of IMQ-induced psoriasis, IL-17 and IL-22 produced by Th17 cells induce the expression of a variety of proinflammatory mediators and induce epidermal proliferation<sup>66,67</sup>. In human psoriasis, the number of Th17 cells is elevated, and the level of IL-17 and IL-22 expression correlates with disease severity<sup>68</sup>. The involvement of IL-17 in neutrophil-mediated inflammation suggests that neutrophils may also be involved in the pathogenesis of psoriasis<sup>69</sup>. 5-LOX, predominantly expressed in neutrophils<sup>70</sup>, produces LTB<sub>4</sub>, which then binds to its receptor BLT1 to exert a variety of effects<sup>71</sup>. BLT1 and CXCR2 coordinately promote neutrophil infiltration into psoriatic skin. IL-1 $\beta$  produced by neutrophils then promotes IL-19 production in keratinocytes, leading to acanthosis<sup>51</sup>. The migration of neutrophils in IMQ-induced psoriasis-like skin is reduced in BLT1 knockout mice, and the psoriatic condition is improved<sup>51</sup>. Thus, LTB<sub>4</sub>-BLT1 signaling leads to neutrophil migration and contributes to the induction of psoriatic symptoms<sup>49</sup>. The present results show that RRP inhibited 5-LOX *in vitro* (Fig. 8), suppressed LTB<sub>4</sub> levels *in vivo* (Fig. 14), and reduced epidermal proliferation and



neutrophil infiltration (Fig. 12). These findings suggest that RRP treatment markedly decreases psoriatic symptoms via 5-LOX inhibition.

PGE<sub>2</sub> produced by COX-2 and mPGES-1 binds to the EP2 and EP4 receptors on Th17 cells, driving psoriatic inflammation<sup>72</sup>. It was observed that RRP inhibited mPGES-1, the terminal enzyme in PGE<sub>2</sub> synthesis, but increased the production of the proinflammatory lipid mediators PGE<sub>2</sub> and PGD<sub>2</sub> (Fig. 14). Because of the dominant effect of 5-LOX inhibition by RRP, COX likely plays a role in maintaining the metabolic balance in this pathway. Although the value of RRP inhibition of mPGES-1 *in vivo* is yet unproven, these observations suggest that RRP may exert therapeutic activity on psoriatic inflammation.

While recent studies have reported the amelioration of IMQ-induced psoriasis-like skin by the phytochemicals paeoniflorin<sup>73,74</sup>, isoflavone<sup>75</sup>, rhododendrin<sup>59</sup>, epigallocatechin-3-gallate<sup>76</sup>, and curcumin<sup>77</sup>, none of the reports elucidate the mechanism underlying the observed effects on psoriatic inflammation. This is the first report that a natural compound improves psoriatic inflammation by decreasing the production of LTB<sub>4</sub> by 5-LOX. In fact, RRP not only inhibited 5-LOX without a chelating effect but also decreased LTB<sub>4</sub> release from intact RBL-2H3 cells (Fig. 8, 9, 11). While the absorption efficiency and pharmacokinetics of RRP remain unknown, the bioavailability of proanthocyanidin has been addressed in several reports. Using an *ex vivo* gut lumen model, S. Deprez *et al.* observed that the proanthocyanidin polymer can be absorbed into the luminal epithelium<sup>78</sup>. T. Shoji *et al.* report that the apple procyanidin, including the octamer, is absorbed and can be detected in plasma after oral administration of apple procyanidin oligomers to rats<sup>79</sup>. In the present findings, similar *in vitro* inhibition of 5-LOX by catechin monomer and RRP (catechin octamer) was observed. However, the

monomer was not effective in decreasing symptoms in the psoriasis-like skin model *in vivo*, indicating that the catechin octamer is more useful than the monomer as a therapeutic agent. The IC<sub>50</sub> of RRP for 5-LOX inhibition (7  $\mu$ M) (Fig. 8A) is comparable to that of several known 5-LOX inhibitors, including baicalein <sup>80</sup>, oleuropein <sup>81</sup>, and eupatilin <sup>82</sup>. However, few studies address inhibition patterns and *in vivo* studies, and none address the possible calcium ion chelating effect of these compounds. In this study, the findings ruled out the possibility of such an effect by RRP (Fig. 9).

## **Chapter IV**

### **Conclusion Remarks**

PGE<sub>2</sub> and LTs are the most important pro-inflammatory lipid mediators among eicosanoids. They induce acute inflammation, and if the effects are excessive and sustained they make chronic inflammatory disorders including dermatitis, asthma, cancer, and neurodegeneration. Preventing chronic inflammation, the medication inhibiting PGE<sub>2</sub> and LTs production is considered important. Actually, NSAIDs are used clinically as COX inhibitors to decrease PGE<sub>2</sub> production, but they have gastrointestinal and cardiovascular side-effects. Zileuton, 5-LOX inhibitor, also has problems such as liver toxicity. It is truly significant to explore the substances without side effects. In the present study, some compounds derived from natural products were found.

Ellagitannins isolated from pomegranate leaves, granatin A and granatin B, and the structural analog, geraniin, selectively suppressed mPGES-1 expression without affecting COX-2 in non-small cell lung carcinoma A549 cells. The ellagitannins also down-regulated TNF $\alpha$ , iNOS, and anti-apoptotic factor Bcl-2, and induced A549 cells to undergo apoptosis. These findings indicate that the ellagitannins may have anti-inflammatory and anti-carcinogenic effects, due to their specific suppression of mPGES-1 without side effects by COX inhibition.

Proanthocyanidin isolated from red-kerneled rice inhibited mPGES-1 (IC<sub>50</sub> 7.7  $\mu$ M) with noncompetitive inhibition and 5-LOX (IC<sub>50</sub> 9.0  $\mu$ M) with mixed noncompetitive inhibition. The proanthocyanidin decreased PGE<sub>2</sub> and LTB<sub>4</sub> production in A549 cells and RBL-2H3 cells, respectively. In IMQ-induced psoriasis-like mouse skin which LTB<sub>4</sub> is deeply involved, a topical application of the proanthocyanidin significantly decreased LTB<sub>4</sub> production in the skin causing to suppress hyperplasia, decrease inflammatory cell infiltration, and down-regulate the psoriasis-associated genes. These results increase our understanding of the mechanism underlying the anti-inflammatory

effect of the proanthocyanidin. The compound may prove to have therapeutic effects on 5-LOX and/or LT-related disorders.

Taken together, this study reveals that pomegranate leaf-derived ellagitannins and red-kerneled rice-derived proanthocyanidin have inhibitory mechanism of pro-inflammatory lipid mediator synthesis and function for prevention or improvement of chronic inflammation.

## Acknowledgement

The completion of this doctoral dissertation is owing to the support of the following persons.

I would like to gratefully and sincerely thank my supervisor, Prof. Toshiko Yamamoto for her support and encouragement during the course of this study. I also greatly appreciate to Prof. Yoshitaka Takahashi, Prof. Hideyuki Ito, Prof. Tetsuya Ogino, Prof. Jinro Takato and Assoc. prof. Yuki Kawakami for their warm supports and advice.

I owe my deepest gratitude to Dr. Izumi Tsukayama and all students who are/were present in Prof. Yamamoto's laboratory for their supports and friendships.

I am grateful to Prof. Hideyuki Ito, Dr. Natsuki Ganeko for providing samples derived from natural products.

I would like to sincerely thank Prof. Makoto Murakami and Dr. Yoshimi Miki at the University of Tokyo and Assoc. prof. Kei Yamamoto at the Tokushima University for analysis of ESI-MS and advice about this study.

I would like to acknowledge all of the teachers in the Department of Nutritional Science, Faculty of Health and Welfare Science, Okayama Prefectural University for their positive helps and supports.

Finally, I would like to express my hearty thanks to my friends and family.

## References

1. Shimizu, T. & Wolfe, L. S. Arachidonic acid cascade and signal transduction. *J. Neurochem.* **55**, 1–15 (1990).
2. Samuelsson, B., Morgenstern, R. & Jakobsson, P. J. Membrane prostaglandin E synthase-1: a novel therapeutic target. *Pharmacol. Rev.* **59**, 207–224 (2007).
3. Sugimoto, Y. & Narumiya, S. Prostaglandin E receptors. *J. Biol. Chem.* **282**, 11613–11617 (2007).
4. Narumiya, S., Sugimoto, Y., Ushikubi, F. & Conclusions, V. I. Prostanoid receptors: structures, properties, and functions. *Physiol Rev.* **79**, 1193–1226 (1999).
5. Murakami, M., Naraba, H., Tanioka, T., Semmyo, N., Nakatani, Y., Kojima, F., Ikeda, T., Fueki, M., Ueno, A., Oh-ishi, S. & Kudo, I. Regulation of prostaglandin E<sub>2</sub> biosynthesis by inducible membrane-associated prostaglandin E<sub>2</sub> synthase that acts in concert with cyclooxygenase-2. *J. Biol. Chem.* **275**, 32783–32792 (2000).
6. Korotkova, M. & Jakobsson, P. J. Characterization of microsomal prostaglandin E synthase 1 inhibitors. *Basic Clin. Pharmacol. Toxicol.* **114**, 64–69 (2014).
7. Colin, D. F. & Garret, A. F. COX-2 inhibitors and cardiovascular risk. *J. Cardiovasc. Pharmacol.* **50**, 470–479 (2007).
8. Tilo, G., Susanne, F. & Garret, A. F. Biological basis for the cardiovascular consequences of COX-2 inhibition: therapeutic challenges and opportunities. *J. Clin. Invest.* **116**, 4–15 (2006).
9. Garret, A. F. Coxibs and cardiovascular disease. *N. Engl. J. Med.* **351**, 1709–1711 (2004).
10. Cheng, Y., Wang, M., Yu, Y., Lawson, J., Funk, C. D. & Fitzgerald, G. A. Cyclooxygenases, microsomal prostaglandin E synthase-1, and cardiovascular function. *J. Clin. Invest.* **116**, 1391–1399 (2006).
11. Suzuki-Yamamoto, T., Tanaka, S., Tsukayama, I., Takafuji, M., Hanada, T., Arakawa, T., Kawakami, Y., Kimoto, M. & Takahashi, Y. *Dioscorea japonica* extract down-regulates prostaglandin E<sub>2</sub> synthetic pathway and induces apoptosis in lung cancer cells. *J. Clin. Biochem. Nutr.* **55**, 162–167 (2014).
12. Tsukayama, I., Toda, K., Takeda, Y., Mega, T., Tanaka, M., Kawakami, Y., Takahashi, Y., Kimoto, M., Yamamoto, K., Miki, Y., Murakami, M. & Suzuki-Yamamoto, T. Preventive effect of *Dioscorea japonica* on squamous cell carcinoma of mouse skin involving down-regulation of prostaglandin E<sub>2</sub> synthetic

- pathway. *J. Clin. Biochem. Nutr.* **62**, 139–147 (2018).
13. Berger, W., De Chandt, M. T. & Cairns, C. B. Zileuton: clinical implications of 5-Lipoxygenase inhibition in severe airway disease. *Int. J. Clin. Pract.* **61**, 663–676 (2007).
  14. Garcia-Marcos, L., Schuster, A. & Perez-Yarza, E. G. Benefit-risk assessment of antileukotrienes in the management of asthma. *Drug Saf.* **26**, 483–518 (2003).
  15. Toda, K., Ueyama, M., Tanaka, S., Tsukayama, I., Mega, T., Konoike, Y., Tamenobu, A., Bastian, F., Akai, I., Ito, H., Kawakami, Y., Takahashi, Y. & Suzuki-Yamamoto, T. Ellagitannins from *Punica granatum* leaves suppress microsomal prostaglandin E synthase-1 expression and induce lung cancer cells to undergo apoptosis. *Biosci. Biotechnol. Biochem.* **84**, 757–763 (2020).
  16. Toda, K., Tsukayama, I., Nagasaki, Y., Konoike, Y., Tamenobu, A., Ganeko, N., Ito, H., Kawakami, Y., Takahashi, Y., Miki, Y., Yamamoto, K., Murakami, M. & Suzuki-Yamamoto, T. Red-kerneled rice proanthocyanidin inhibits arachidonate 5-lipoxygenase and decreases psoriasis-like skin inflammation. *Arch. Biochem. Biophys.* in press.
  17. Wang, R., Ding, Y., Liu, R., Xiang, L. & Du, L. Pomegranate: Constituents, bioactivities and pharmacokinetics. *Fruit, Veg. Cereal Sci. Biotechnol.* **4**, 77–87 (2010).
  18. Ismail, T., Sestili, P. & Akhtar, S. Pomegranate peel and fruit extracts: A review of potential anti-inflammatory and anti-infective effects. *J. Ethnopharmacol.* **143**, 397–405 (2012).
  19. Pinheiro, A. J. M. C. R., Goncalves, J. S., Dourado, A. W. A., de Sousa, E. M., Brito, N. M., Silva, L. K., Batista, M. C. A., de Sa, J. C., Monteiro, C. R. A. V., Fernandes, E. S., Monteiro-Neto, V., Campbell, L. A., Zago, P. M. W. & Lima-Neto, L. G. *Punica granatum* L. leaf extract attenuates lung inflammation in mice with acute lung injury. *J. Immunol. Res.* **2018**, 6879183 (2018).
  20. Marques, L. C. F., Pinheiro, A. J. M. C. R., Araujo, J. G. G., de Oliveira, R. A. G., Silva, S. N., Abreu, I. C., de Sousa, E. M., Fernandes, E. S., Luchessi, A. D., Silbiger, V. N., Nicolete, R. & Lima-Neto, L. G. Anti-inflammatory effects of a pomegranate leaf extract in LPS-induced peritonitis. *Planta Med.* **82**, 1463–1467 (2016).
  21. Tanaka, T., Nonaka, G. & Nishioka, I. Tannins and related compounds. C. Reaction of dehydrohexahydroxydiphenic acid esters with bases, and its application to the structure determination of pomegranate tannins, granatins A and B. *Chem. Pharm. Bull.* **38**, 2424–2428 (1990).



22. Okuda, T., Hatano, T., Nitta, H. & Fujii, R. Hydrolysable tannins having enantiomeric dehydrohexahydroxydiphenoyl group: Revised structure of terchebin and structure of granatin B. *Tetrahedron Lett.* **21**, 4361–4364 (1980).
23. Ito, H., Hatano, T., Namba, O., Shirono, T., Okuda, T. & Yoshida, T. Constituents of *Geranium thunbergii* SIEB. et ZUCC. XV. modified dehydroellagitannins, geraniinic acids B and C, and phyllanthusiin F. *Chem. Pharm. Bull.* **47**, 1148–1151 (1999).
24. Haddock, E. A., Gupta, R. K. & Haslam, E. The metabolism of gallic acid and hexahydroxydiphenic acid in plants. Part 3. Esters of (R)- and (S)-hexahydroxydiphenic acid and dehydrohexahydroxydiphenic acid with D-glucopyranose ( $^1C_4$  and related conformations). *J. Chem. Soc. Perkin Trans. I* 2535–2545 (1982).
25. Tanaka, T., Nonaka, G. & Nishioka, I. Punicafolin, an ellagitannin from the leaves of *Punica granatum*. *Phytochemistry* **24**, 2075–2078 (1985).
26. Okuda, T. & Yoshida, T.  $^{13}C$  Nuclear Magnetic Resonance Spectra of Corilagin and Geraniin. *Heterocycles* **14**, 1743–1749 (1980).
27. Ito, H. Metabolites of the ellagitannin geraniin and their antioxidant activities. *Planta Med.* **77**, 1110–1115 (2011).
28. Bastian, F., Ito, Y., Ogahara, E., Ganeko, N., Hatano, T. & Ito, H. Simultaneous quantification of ellagitannins and related polyphenols in *geranium thunbergii* using quantitative NMR. *Molecules* **23**, 1346 (2018).
29. Feldman, K. S. Recent progress in ellagitannin chemistry. *Phytochemistry* **66**, 1984–2000 (2005).
30. Lee, C. J., Chen, L. G., Liang, W. L. & Wang, C. C. Anti-inflammatory effects of *punica granatum* linne *in vitro* and *in vivo*. *Food Chem.* **118**, 315–322 (2010).
31. Ding, Y., Tong, M., Liu, S., Moscow, J. A. & Tai, H. H. NAD<sup>+</sup>-linked 15-hydroxyprostaglandin dehydrogenase (15-PGDH) behaves as a tumor suppressor in lung cancer. *Carcinogenesis* **26**, 65–72 (2005).
32. Jin, Z., Yu, Y., Jin, R. H., Wang, Y. B. & Xu, H. Y. Effect of granatin B on the glioma cancer by inducing apoptosis. *Am. J. Transl. Res.* **8**, 3970–3975 (2016).
33. Li, J., Wang, S., Yin, J. & Pan, L. Geraniin induces apoptotic cell death in human lung adenocarcinoma A549 cells *in vitro* and *in vivo*. *Can. J. Physiol. Pharmacol.* **91**, 1016–1024 (2013).
34. Sedger, L. M. & McDermott, M. F. TNF and TNF-receptors: From mediators of cell death and inflammation to therapeutic giants – past, present and future. *Cytokine Growth Factor Rev.* **25**, 453–472 (2014).

35. Nie, M., Pang, L., Inoue, H. & Knox, A. J. Transcriptional regulation of cyclooxygenase 2 by bradykinin and interleukin-1 $\beta$  in human airway smooth muscle cells: involvement of different promoter elements, transcription factors, and histone H4 acetylation. *Mol. Cell. Biol.* **23**, 9233–9244 (2003).
36. Kang, Y. J., Wingerd, B. A., Arakawa, T. & Smith, W. L. Cyclooxygenase-2 gene transcription in a macrophage model of inflammation. *J. Immunol.* **177**, 8111–8122 (2006).
37. Naraba, H., Yokoyama, C., Tago, N., Murakami, M., Kudo, I., Fueki, M., Oh-Ishi, S. & Tanabe, T. Transcriptional regulation of the membrane-associated prostaglandin E<sub>2</sub> synthase gene. Essential role of the transcription factor Egr-1. *J. Biol. Chem.* **277**, 28601–28608 (2002).
38. Moon, Y., Glasgow, W. C. & Eling, T. E. Curcumin suppresses interleukin 1 $\beta$ -mediated microsomal prostaglandin E synthase 1 by altering early growth response gene 1 and other signaling pathways. *J. Pharmacol. Exp. Ther.* **315**, 788–795 (2005).
39. Zhou, J., Joplin, D. G., Cross, J. V & Templeton, D. J. Sulforaphane inhibits prostaglandin E<sub>2</sub> synthesis by suppressing microsomal prostaglandin E synthase 1. *PLoS One* **7**, 1–12 (2012).
40. Zhou, H., Liu, J. X., Luo, J. F., Cheng, C. S., Leung, E. L. H., Li, Y., Su, X. H., Liu, Z. Q., Chen, T. B., Duan, F. G., Dong, Y., Zuo, Y. H., Li, C., Lio, C. K., Li, T., Luo, P., Xie, Y., Yao, X. J., Wang, P. X. & Liu, L. Suppressing mPGES-1 expression by sinomenine ameliorates inflammation and arthritis. *Biochem. Pharmacol.* **142**, 133–144 (2017).
41. Desai, S. J., Prickril, B. & Rasooly, A. Mechanisms of phytonutrient modulation of cyclooxygenase-2 (COX-2) and inflammation related to cancer. *Nutr. Cancer* **70**, 350–375 (2018).
42. Abdel-Aal, E.-S. M., Young, J. C. & Rabalski, I. Anthocyanin composition in black, blue, pink, purple, and red cereal grains. *J. Agric. Food Chem.* **54**, 4696–4704 (2006).
43. Ganeko, N., Kato, N., Watanabe, S., Bastian, F., Miyake, M. & Ito, H. Proanthocyanidin and anthocyanins from the hulls and beards of red-kerneled rice and their antiglycation properties. *Biosci. Biotechnol. Biochem.* **83**, 605–608 (2019).
44. Gunaratne, A., Wu, K., Li, D., Bentota, A., Corke, H. & Cai, Y.-Z. Antioxidant activity and nutritional quality of traditional red-grained rice varieties containing proanthocyanidins. *Food Chem.* **138**, 1153–1161 (2013).

45. Limtrakul, P., Yodkeeree, S., Pitchakarn, P. & Punfa, W. Anti-inflammatory effects of proanthocyanidin-rich red rice extract via suppression of MAPK, AP-1 and NF- $\kappa$ B pathways in Raw 264.7 macrophages. *Nutr. Res. Pract.* **10**, 251–258 (2016).
46. Krueger, J. G. & Bowcock, A. Psoriasis pathophysiology: current concepts of pathogenesis. *Ann. Rheum. Dis.* **64**, ii30–ii36 (2005).
47. Zheng, Y., Danilenko, D. M., Valdez, P., Kasman, I., Eastham-Anderson, J., Wu, J. & Ouyang, W. Interleukin-22, a Th17 cytokine, mediates IL-23-induced dermal inflammation and acanthosis. *Nature* **445**, 648–651 (2007).
48. Albanesi, C., Scarponi, C., Bosisio, D., Sozzani, S. & Girolomoni, G. Immune functions and recruitment of plasmacytoid dendritic cells in psoriasis. *Autoimmunity* **43**, 215–219 (2010).
49. Iversen, L., Kragballe, K. & Ziboh, V. A. Significance of leukotriene-A<sub>4</sub> hydrolase in the pathogenesis of psoriasis. *Skin Pharmacol.* **10**, 169–177 (1997).
50. Honda, T. & Kabashima, K. Prostanoids and leukotrienes in the pathophysiology of atopic dermatitis and psoriasis. *Int. Immunol.* **31**, 589–595 (2019).
51. Sumida, H., Yanagida, K., Kita, Y., Abe, J., Matsushima, K., Nakamura, M., Ishii, S., Sato, S. & Shimizu, T. Interplay between CXCR2 and BLT1 facilitates neutrophil infiltration and resultant keratinocyte activation in a murine model of imiquimod-induced psoriasis. *J. Immunol.* **192**, 4361–4369 (2014).
52. van der Fits, L., Mourits, S., Voerman, J. S., Kant, M., Boon, L., Laman, J. D., Cornelissen, F., Mus, A. M., Florencia, E., Prens, E. P. & Lubberts, E. Imiquimod-induced psoriasis-like skin inflammation in mice is mediated via the IL-23/IL-17 axis. *J. Immunol.* **182**, 5836–5845 (2009).
53. Kawakami, Y., Hosokawa, T., Morinaka, T., Irino, S., Hirano, S., Kobayashi, H., Yoshioka, A., Suzuki-Yamamoto, T., Yokoro, M., Kimoto, M., Tsuji, H., Yamashita, H., Doi, S., Yutani, C., Kato, R., Itabe, H., Kanada, T., Hada, T. & Takahashi, Y. Antiatherogenic effect of guava leaf extracts inhibiting leucocyte-type 12-lipoxygenase activity. *Food Chem.* **131**, 1069–1075 (2012).
54. Kawakami, Y., Nakamura, T., Hosokawa, T., Suzuki-Yamamoto, T., Yamashita, H., Kimoto, M., Tsuji, H., Yoshida, H., Hada, T. & Takahashi, Y. Antiproliferative activity of guava leaf extract via inhibition of prostaglandin endoperoxide H synthase isoforms. *Prostaglandins Leukot. Essent. Fat. Acids* **80**, 239–245 (2009).
55. Suzuki, H., Miyauchi, D. & Yamamoto, S. A selective inhibitor of arachidonate 5-lipoxygenase scavenging peroxide activator. *Biochem. Pharmacol.* **54**, 529–532 (1997).

56. Sakashita, T., Takahashi, Y., Kinoshita, T. & Yoshimoto, T. Essential involvement of 12-lipoxygenase in regiospecific and stereospecific oxidation of low density lipoprotein by macrophages. *Eur. J. Biochem.* **265**, 825–831 (1999).
57. Kinoshita, T., Takahashi, Y., Sakashita, T., Inoue, H., Tanabe, T. & Yoshimoto, T. Growth stimulation and induction of epidermal growth factor receptor by overexpression of cyclooxygenases 1 and 2 in human colon carcinoma cells. *Biochim. Biophys. Acta* **1438**, 120–130 (1999).
58. Reagan-Shaw, S., Nihal, M. & Ahmad, N. Dose translation from animal to human studies revisited. *FASEB J.* **22**, 659–661 (2008).
59. Jeon, Y.-J., Sah, S. K., Yang, H. S., Lee, J. H., Shin, J. & Kim, T.-Y. Rhododendrin inhibits toll-like receptor-7-mediated psoriasis-like skin inflammation in mice. *Exp. Mol. Med.* **49**, e349 (2017).
60. Yamamoto, K., Miki, Y., Sato, H., Murase, R., Taketomi, Y. & Murakami, M. Secreted phospholipase A<sub>2</sub> specificity on natural membrane phospholipids. *Methods Enzym.* **583**, 101–117 (2017).
61. Bligh, E. G. & Dyer, W. J. A rapid method of total lipid extraction and purification. *Can. J. Biochem. Physiol.* **37**, 911–917 (1959).
62. Yamamoto, K., Miki, Y., Sato, M., Taketomi, Y., Nishito, Y., Taya, C., Muramatsu, K., Ikeda, K., Nakanishi, H., Taguchi, R., Kambe, N., Kabashima, K., Lambeau, G., Gelb, M. H. & Murakami, M. The role of group IIF-secreted phospholipase A<sub>2</sub> in epidermal homeostasis and hyperplasia. *J. Exp. Med.* **212**, 1901–1919 (2015).
63. Jakschik, B. A. & Lee, L. H. Enzymatic assembly of slow reacting substance. *Nature* **287**, 51–52 (1980).
64. Shimizu, T., Izumi, T., Seyama, Y., Tadokoro, K., Radmark, O. & Samuelsson, B. Characterization of leukotriene A<sub>4</sub> synthase from murine mast cells: evidence for its identity to arachidonate 5-lipoxygenase. *Proc. Natl. Acad. Sci. U. S. A.* **83**, 4175–4179 (1986).
65. Rouzer, C. A. & Kargman, S. Translocation of 5-lipoxygenase to the membrane in human leukocytes challenged with ionophore A23187. *J. Biol. Chem.* **263**, 10980–10988 (1988).
66. Nickoloff, B. J. Cracking the cytokine code in psoriasis. *Nature medicine* **13**, 242–244 (2007).
67. Perera, G. K., Di Meglio, P. & Nestle, F. O. Psoriasis. *Annu. Rev. Pathol.* **7**, 385–422 (2012).
68. Johnson-Huang, L. M., Suárez-Fariñas, M., Sullivan-Whalen, M., Gilleaudeau, P., Krueger, J. G. & Lowes, M. A. Effective narrow-band UVB radiation therapy

- suppresses the IL-23/IL-17 axis in normalized psoriasis plaques. *J. Invest. Dermatol.* **130**, 2654–63 (2010).
69. Pelletier, M., Maggi, L., Micheletti, A., Lazzeri, E., Tamassia, N., Costantini, C., Cosmi, L., Lunardi, C., Annunziato, F., Romagnani, S. & Cassatella, M. A. Evidence for a cross-talk between human neutrophils and Th17 cells. *Blood* **115**, 335–343 (2010).
  70. Brock, T. G., Paine, R. & Peters-Golden, M. Localization of 5-lipoxygenase to the nucleus of unstimulated rat basophilic leukemia cells. *J. Biol. Chem.* **269**, 22059–66 (1994).
  71. Yokomizo, T., Izumi, T., Chang, K., Takuwa, Y. & Shimizu, T. A G-protein-coupled receptor for leukotriene B<sub>4</sub> that mediates chemotaxis. *Nature* **387**, 620–624 (1997).
  72. Lee, J., Aoki, T., Thumkeo, D., Siriwach, R., Yao, C. & Narumiya, S. T cell–intrinsic prostaglandin E<sub>2</sub> -EP2/EP4 signaling is critical in pathogenic Th17 cell–driven inflammation. *J. Allergy Clin. Immunol.* **143**, 631–643 (2019).
  73. Zhao, J., Di, T., Wang, Y., Wang, Y., Liu, X., Liang, D. & Li, P. Paeoniflorin inhibits imiquimod-induced psoriasis in mice by regulating Th17 cell response and cytokine secretion. *Eur. J. Pharmacol.* **772**, 131–143 (2016).
  74. Sun, Y., Zhang, J., Huo, R., Zhai, T., Li, H., Wu, P., Zhu, X., Zhou, Z., Shen, B. & Li, N. Paeoniflorin inhibits skin lesions in imiquimod-induced psoriasis-like mice by downregulating inflammation. *Int. Immunopharmacol.* **24**, 392–399 (2015).
  75. Li, H.-J., Wu, N.-L., Lee, G.-A. & Hung, C.-F. The therapeutic potential and molecular mechanism of isoflavone extract against psoriasis. *Sci. Rep.* **8**, 6335 (2018).
  76. Chamcheu, J. C., Siddiqui, I. A., Adhami, V. M., Esnault, S., Bharali, D. J., Babatunde, A. S., Adame, S., Massey, R. J., Wood, G. S., Longley, B. J., Mousa, S. A. & Mukhtar, H. Chitosan-based nanoformulated (-)-epigallocatechin-3-gallate (EGCG) modulates human keratinocyte-induced responses and alleviates imiquimod-induced murine psoriasiform dermatitis. *Int. J. Nanomedicine* **13**, 4189–4206 (2018).
  77. Sun, J., Zhao, Y. & Hu, J. Curcumin inhibits imiquimod-induced psoriasis-like inflammation by inhibiting IL-1 $\beta$  and IL-6 production in mice. *PLoS One* **8**, e67078 (2013).
  78. Deprez, S., Mila, I., Huneau, J.-F., Tome, D. & Scalbert, A. Transport of proanthocyanidin dimer, trimer, and polymer across monolayers of human

- intestinal epithelial Caco-2 cells. *Antioxid. Redox Signal.* **3**, 957–967 (2001).
79. Shoji, T., Masumoto, S., Moriichi, N., Akiyama, H., Kanda, T., Ohtake, Y. & Goda, Y. Apple procyanidin oligomers absorption in rats after oral administration: Analysis of procyanidins in plasma using the porter method and high-performance liquid chromatography/tandem mass spectrometry. *J. Agric. Food Chem.* **54**, 884–892 (2006).
80. Furukawa, M., Yoshimoto, T., Ochi, K. & Yamamoto, S. Studies on arachidonate 5-lipoxygenase of rat basophilic leukemia cells. *Biochim. Biophys. Acta* **795**, 458–465 (1984).
81. Kohyama, N., Nagata, T., Fujimoto, S. & Sekiya, K. Inhibition of arachidonate lipoxygenase activities by 2-(3,4-dihydroxyphenyl)ethanol, a phenolic compound from olives. *Biosci. Biotechnol. Biochem.* **61**, 347–350 (1997).
82. Koshihara, Y., Neichi, T., Murota, S., Lao, A., Fujimoto, Y. & Tatsuno, T. Selective inhibition of 5-lipoxygenase by natural compounds isolated from Chinese plants, *Artemisia rubripes* Nakai. *FEBS Lett.* **158**, 41–44 (1983).